Glacial-interglacial trench supply variation, spreading-ridge subduction, and feedback controls on the Andean margin development at the Chile triple junction area (45-48°S)

Jacques Bourgois, Christèle Guivel, Yves Lagabrielle, Thierry Calmus, Jacques Boulègue, Valérie Daux

JOURNAL OF GEOPHYSICAL RESEARCH, VOL. 105, NO. B4, PAGES 8355–8386, APRIL 10, 2000

Glacial-interglacial trench supply variation, spreading-ridge subduction, and feedback controls on the Andean margin development at the Chile triple junction area (45-48°S)

Jacques Bourgois,[1] Christèle Guivel,[2] Yves Lagabrielle,[3] Thierry Calmus,[4] Jacques Boulègue,[5] and Valérie Daux[6]

Abstract. During the Chile triple junction (CTJ) cruise (March-April 1997), EM12 bathymetry and seismic reflection data were collected in the vicinity of the Chile triple junction (45-48°S), where an active spreading ridge is being subducted beneath the Andean continental margin. Results show a continental margin development shaped by tectonic processes spanning a spectrum from subduction-erosion to subduction-accretion. The Andean continental margin and the Chile trench exhibit a strong segmentation which reflects the slab segmentation and the Chile triple junction migration. Three segments were identified along the Andean continental margin: the presubduction, the synsubduction, and the postsubduction segments, from north to south. Both climate-induced variations of the sediment supply to the trench and the tectonic reorganization at the Nazca-Antarctica plate boundary involving postsubduction ridge jump are the two main factors that control the tectonic regime of this continental margin. Along the survey area we infer the succession of two different periods during the last glacial-interglacial cycle: a glacial period with ice-rafted detrital discharges restricted to the shoreline area and low river output and a warmer period during which the Andean ice cap retreat allowed the Andes to be drained off. During these warm periods, rapid increase in trench deposition caused the margin to switch from subduction-erosion or nonaccretion to subduction-accretion: (1) along the presubduction segment after the last deglaciation and (2) along the postsubduction segment after the interglacial episode at 130-117 ka. Conversely, a nonaccretion or subduction-erosion mode characterized the presubduction and postsubduction segments during glacial maximums. The major effects of subduction of the buoyant Chile ridge include a shallow trench which diverts trench sediment supply and tectonic instabilities at the Nazca-Antarctica plate boundary. We suggest that a postsubduction westward jump of the Chile ridge occurred during the past 780 kyr. It produced slab fragmentation and individualization of an ephemeral microplate north of the Taitao fracture zone: the Chonos microplate. In 780 kyr, two episodes of subduction-accretion separated by an episode of subduction-erosion occurred in relation with the Chonos microplate individualization and subduction. The current northward migration of the triple junction along the Chonos microplate-South America plate boundary introduces a sharp change in the tectonic mode from subduction-erosion to the north to subduction-accretion to the south. The data collected along the Taitao ridge have revealed the complex three-dimensional structure of an accretionary wedge which includes a midslope thrust sheet exhibiting the characteristics of an ophiolite: the Taitao Ridge ophiolite. No connection exists between the Taitao Ridge ophiolite and the Bahia Barrientos ophiolite cropping out onland in the Taitao peninsula.

[1]Centre National de la Recherche Scientifique, Université Pierre et Marie Curie, Laboratoire de Géodynamique, Tectonique et Environnement, Paris.

[2]Laboratoire de Planétologie et Géodynamique, Université de Nantes, Nantes, France

[3]Institut de Recherche pour le Développement, Noumea, Nueva Caledonia

[4]Instituto Geologico, Universidad Autonoma de Mexico, Estacion Regional del Noroeste, Hermosillo, Sonora, Mexico.

[5]Laboratoire de Géochimie et Métallogénie, Université Pierre et Marie Curie, Paris.

[6]Laboratoire de Géologie Sédimentaire, Université Pierre et Marie Curie, Paris.

Paper number 1999JB900400.
0148-0227/00/1999JB900400$09.00

1. Introduction

The Chile triple junction (Figure 1) is the site where the Antarctica, the Nazca and the South America plates meet [*Cande and Leslie*, 1986; *Cande et al.*, 1987; *Behrmann et al.*, 1994]. At 46°09'S, the active spreading center at the Antarctic-Nazca plate boundary is being subducted beneath the South America continental margin. The Chile margin triple junction area provides the opportunity to study the petrological and tectonic effects of spreading ridge subduction along a continental margin, a process that has dramatically affected the geology of both North and South American margins during the past 70 Myr [*Atwater*, 1970; *Dickinson and Snyder*, 1979; *Ramos and Kay*, 1992; *Sisson and Pavlis*, 1993; *Kay et al.*, 1993]. Spreading ridge subduction leaves specific structural and stratigraphic signatures, as recently

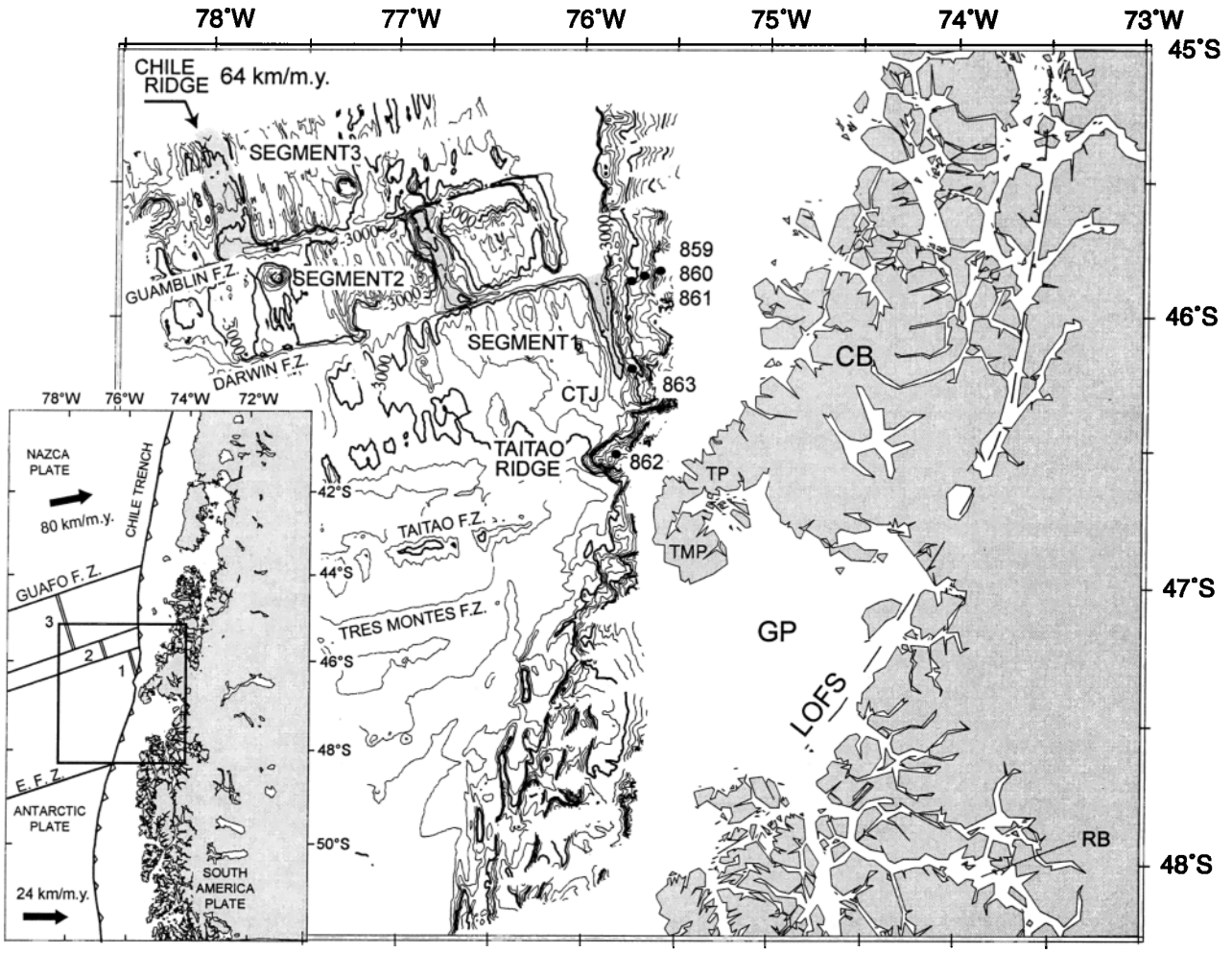

Figure 1. Bathymetric map of the region surveyed during the CTJ cruise of the R/V *L'Atalante* in the Chile triple junction area, between 45°S and 48°S. The main seafloor morphological features include the Chile ridge axes and fracture zones, the Chile trench, and the Andean continental margin. Location map is shown in the inset. Numbers 859 to 863 refer to the ODP sites drilled during ODP Leg 141. Chile triple junction (CTJ); Chiloe block (CB); Esmeralda fracture zone (EFZ); Golfo de Penas (GP); Liquine-Ofqui fault system (LOFS); Rio Baker (RB); Tres Montes peninsula (TMP); Taitao peninsula (TP).

shown along the Taitao peninsula transect, including (1) rapid uplift and subsidence of the forearc domain [*Cande and Leslie*, 1986; *Bourgois et al.*, 1992], (2) anomalous near-trench and forearc magmatism [*Mpodozis et al.*, 1985; *Kaeding et al.*, 1990; *Lagabrielle et al.*, 1994; *Guivel et al.*, 1999], (3) removal of forearc material from the overriding plate [*Cande and Leslie*, 1986; *Cande et al.*, 1987; *Behrmann et al.*, 1992a and b; *Bourgois et al.*, 1996], and (4) extensional tectonics in relation with a subducted ridge segment at depth [*Murdie et al.*, 1993]. Moreover, ophiolite emplacement [*Forsythe and Nelson*, 1995], elevated thermal gradient [*Cande et al.*, 1987], alteration, diagenesis, and mineralization [*Haeussler et al.*, 1995] of forearc materials are expected as a consequence of hot fluids venting from the subducting spreading ridge.

Results of Ocean Drilling Program (ODP) Leg 141 [*Behrmann et al.*, 1992a; *Lewis et al.*, 1995] suggest that the subduction of the active spreading center of the Chile ridge beneath the South American continent is associated with a major change in the tectonic regime of the continental margin. As the Chile triple junction migrated to the north, the tectonic regime of the margin would have evolved from subduction-erosion to subduction-accretion. Indeed, the rebuilding of an accretionary prism following the partial destruction of the forearc [*Behrmann et al.*, 1994; *Bourgois et al.*, 1996] is associated with the passage of the Chile triple junction along the margin. This situation offers to address the question of relative weight of factors controlling the tectonic regime of convergent margins (i.e. type 1 versus type 2 convergent margin [*von Huene and Scholl*, 1991]) and the evolution through space and time from one type to another. Although, the effects of subduction-erosion have been demonstrated at many convergent margins, the constraints of physical conditions that apply at the front of convergent margins have been poorly investigated [*Scholl et al.*, 1980; *Hussong and Wipperman*, 1981; *Aubouin et al.*, 1984; *von Huene and Lallemand*, 1990]. Parameters such as (1) the rate and direction of relative plate motion, (2) the topography of the subducting plate, and (3) the type and volume of sediment need to be quantified [*von Huene*, 1986].

During the CTJ cruise (March 13 to April 7, 1997) of the

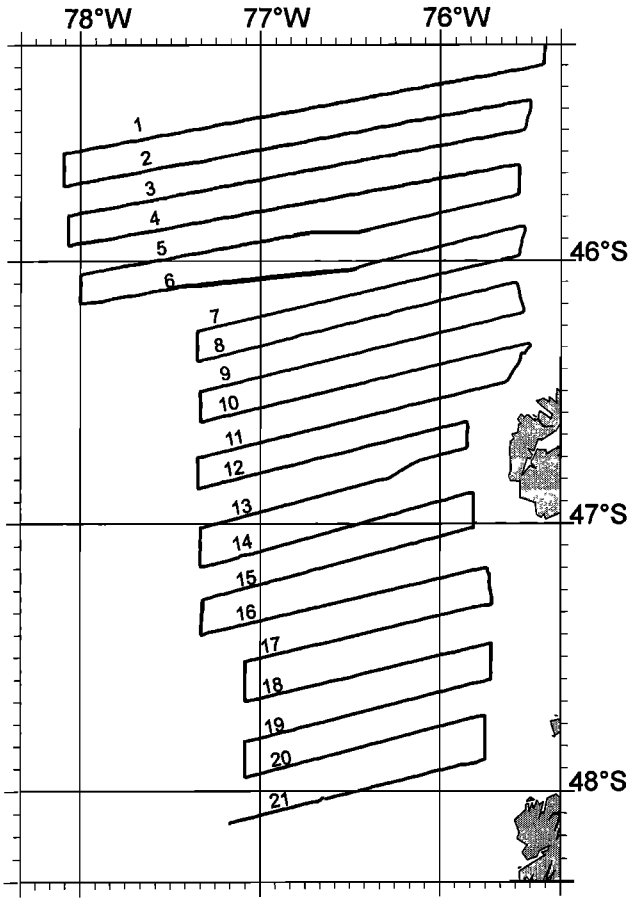

Figure 2. Ship track during the CTJ cruise. Numbers 1 to 21 refer to seismic lines shot during the cruise.

R/V *L'Atalante*, geophysical surveys employing EM12 multibeam echo-sounding, sonar imagery, six-channel seismic reflection, gravity, and magnetic profiling (Figure 2) were conducted in the Chile triple junction area. A 100% coverage bathymetric map (Plate 1) was obtained between 45°S and 48°S [*Bourgois et al.*, 1997]. Samples were collected at numerous dredge sites located in the vicinity of the Chile triple junction on both oceanic and continental sides of the Chile trench.

The Andean continental margin and the Chile trench exhibit a strong segmentation which reflects the slab segmentation in relation with the northward migration of the Chile triple junction. From north to south, three main segments are defined: (1) North of the Darwin fracture zone, the "presubduction segment" which extends from 45°10'S to 45°50'S is representative of the margin before the subduction of the Chile ridge. A thick trench infill underthrusting below a narrow continental slope characterizes this segment. (2) Between 45°50'S and 47°10'S, a very complex segment of the margin is designated as the "synsubduction segment". This segment is divided into three subsegments. From north to south it includes the "Chile ridge subsegment", along which the Chile ridge is currently subducting beneath the continental margin between the Darwin fracture zone and the Chile triple junction; the "North Taitao canyon subsegment", between the Chile triple junction and the South Taitao canyon; and the "Taitao ridge subsegment", located seaward of the Taitao and Tres Montes peninsulas which extends from 46°26'S to 47°S. (3) The typical "postsubduction segment", located south of 47°10'S, exhibits a wide accretionary wedge (i.e., the Golfo de Penas accretionary prism).

Climate-induced variations of the sediment supply to the trench axis and the tectonic reorganization at the Nazca-Antarctica plate boundary involving postsubduction ridge jump are identified as two main factors that control the tectonic regime of the Andean continental margin in the Chile triple junction area. A nonaccretion or subduction-erosion mode characterized the presubduction and postsubduction segments during the two last glacial maximums, whereas warmer periods associated with rapid increase in trench deposition caused the margin to switch from subduction-erosion or nonaccretion to subduction-acccretion. The major effects of subduction of the buoyant Chile ridge include a shallow trench which divert trench sediment supply and tectonic instabilities at the Nazca-Antarctica plate boundary. A postsubduction westward jump of the Chile ridge occurred during the past 780 kyr. It produced slab fragmentation and individualization of an ephemeral microplate. In 780 kyr, two episodes of subduction-accretion separated by an episode of subduction-erosion occurred along the synsubduction segment. The data collected along the Taitao Ridge reveals the complex three-dimensional structure of an accretionary wedge which includes a midslope thrust sheet exhibiting the characteristics of an ophiolite: the Taitao Ridge ophiolite. The survey carried out by the R/V *L'Atalante* helps to better address the problem of mass transfer in the case of the subduction of an active spreading center and examine the main factors determining the tectonic regime of the continental margin.

2. Tectonic Setting

Seafloor spreading along the Chile ridge at the Nazca-Antarctica plate boundary (Figure 1) occurred at a rate of 64 km/Myr [*DeMets et al.*, 1990] over the past 5 Myr [*Herron et al.*, 1981]. North of the Chile triple junction, the Nazca plate is being subducted beneath the South America plate at a rate of 80 km/Myr in a N80°E direction. To the south, the Antarctic plate is subducted beneath the South America plate at a rate of 24 km/Myr in an E-W direction. The South Chile ridge (Plate 1) consists of short segments (segment 1, 2, and 3) trending N160°-165°E, separated by a series of parallel fracture zones. In the area surveyed during the CTJ cruise they are the Darwin and Guamblin fracture zones north of the Chile triple junction and the Taitao and Tres Montes fracture zones to the south. Because the Chile ridge axis is ~10° oblique to the Chile trench axis, the Chile triple junction migrates northward at ~160 km/Myr when in a ridge-trench-trench configuration as today [*Cande et al.*, 1987]. When in a transform-trench-trench configuration, the Chile triple junction migrates slowly back to the south, at a rate of 10 km/Myr.

According to kinematic reconstruction [*Forsythe et al.*, 1986], a long segment of the Chile ridge met with the Chile trench west of Tierra de Fuego, at 52°S, around 14 Ma. The northern section of this segment, bounded to the north by the Esmeralda fracture zone, subducted at about 49°S between 12 and 10 Ma. In the surveyed area the Chile ridge segment located between the Esmeralda and the Tres Montes fracture zones was then subducted around 6 Ma. Off the Taitao and Tres Montes peninsulas, the subduction history was reconstructed in detail by *Leslie* [1986]. From 5-6 to 3 Ma, when the Tres Montes fracture zone subduction occurred, the

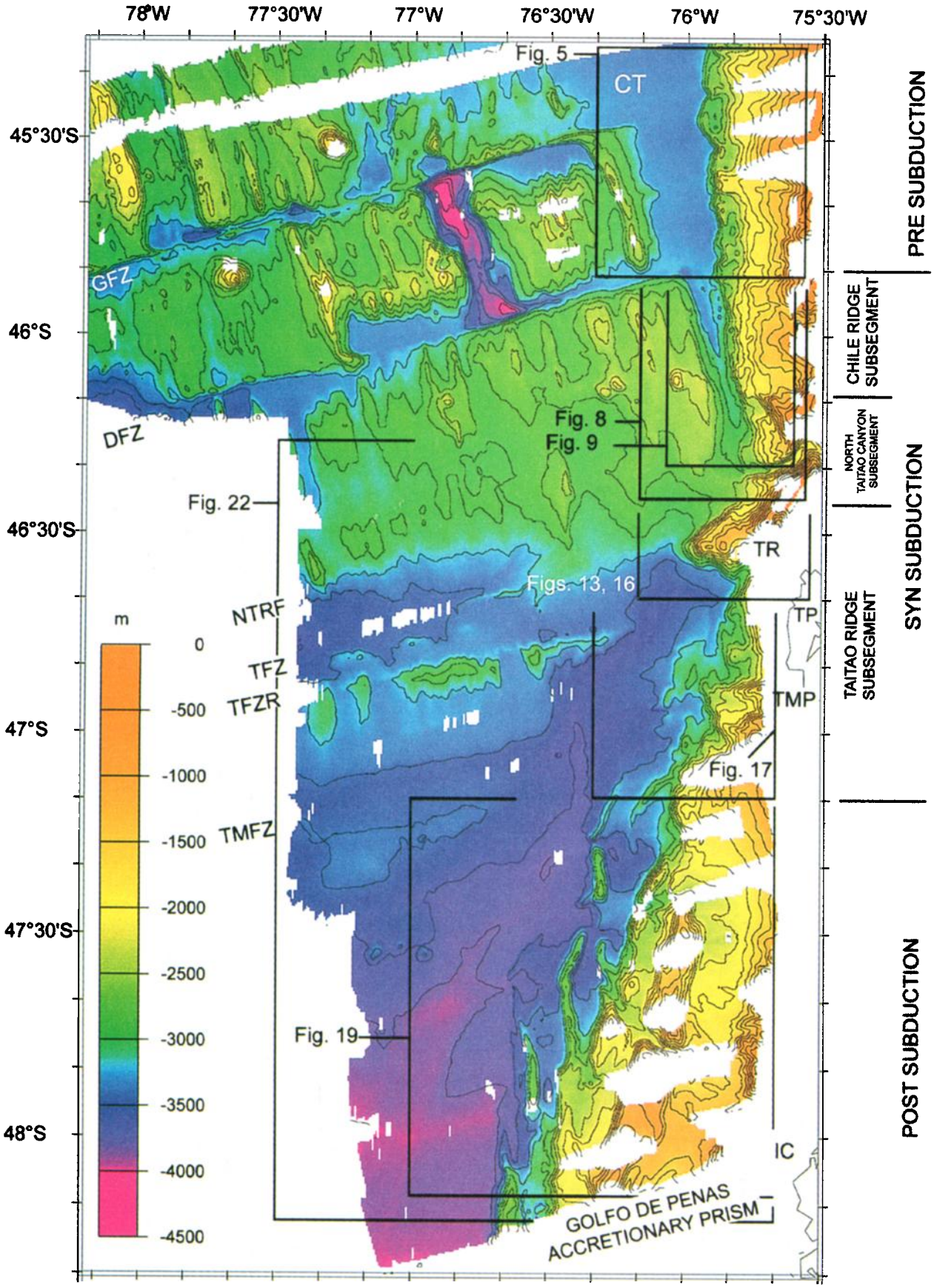

Plate 1. Bathymetry derived from the EM12 data. Scale on the left shows the color code for water depth. Location maps for Figures 5, 8, 9, 13, 16, 17, 19, and 22 are shown. Chile trench (CT); Darwin fracture zone (DFZ); Guamblin fracture zone (GFZ); Isla Campana (IC); North Taitao Ridge fault (NTRF); Taitao fracture zone (TFZ); Taitao Fracture Zone ridge (TFZR); Taitao Ridge (TR); Tres Montes fracture zone (TMFZ); Tres Montes peninsula (TMP); Taitao peninsula (TP).

triple junction migrated to the south from 46°35'S to 46°45'S. From 3 to 2.8 Ma the short ridge segment located between the Tres Montes and Taitao fracture zones was then subducted in association with the northward migration of the triple junction, from 46°35'S to 46°25'S. From 2.8 to 0.2-0.3 Ma the subduction of the Taitao fracture zone occurred in an area located between 46°25'S and 46°30'S. Since 0.2-0.3 Ma the Chile triple junction defined by the ridge segment located north of the Taitao fracture zone (i.e., the Chile ridge segment 1, CRS 1 hereafter) and the trench (Figure 1) migrated northward to its present location, at 46°09'S.

The map pattern of shallow depth (i.e., <100 km) seismicity exhibits a continuous distribution along the Nazca-South America plate boundary as well as along the ridge axis and transforms at the Nazca-Antarctica plate boundary [*Bourgois et al.*, 1993]. Therefore the seismic activity allows *Barazangi and Izacks* [1976] to define accurately the Wadati-Benioff zone north of the triple junction. Between 33°S and 45°S latitude the Nazca slab subducts at an angle of 25-30°. Although much evidence of recent surface faulting has been recognized along the Liquine-Ofqui fault system (Figure 1), the coastal area and the forearc south of the triple junction appear devoid of significant seismic activity. As a consequence, the Antarctica slab geometry beneath the South America plate is poorly defined south of the triple junction. However, *Cande and Leslie* [1986] have proposed that the Antarctica slab is being subducted with an angle of 20° between 46°S and 49°S.

3. Regional Geology

Onland, the most striking features east of the area surveyed during the CTJ cruise between 45°10'S and 48°10'S include (1) the southern end of the right lateral Liquine-Ofqui fault system which bounds the Andean batholith to the west; (2) the calcalkaline South Volcanic Zone whose southern extension is at the latitude of the Chile triple junction at the Mount Hudson volcano. The 46°09'S latitude of the Chile triple junction fits also with the northern boundary of a volcanic gap extending southward to the adakitic Mount Lautaro volcano, at 49°S; and (3) the Chiloe block (Figure 1) west of the Liquine-Ofqui fault system. The geology of the Chiloe block continental margin has been interpreted from both field mapping of onland exposures in the Taitao and Tres Montes peninsulas and ODP Leg 141 drilling.

Impingement of the Chile ridge has caused large-scale deformation of the forearc upper crust. *Forsythe and Nelson* [1985] proposed an indenter kinematic model in which an elongated forearc sliver (the Chiloe block) is moving northward away from an extensional zone located in the Chile triple junction area. Two major tectonic features accommodate this movement: (1) transtensional faults in the Golfo de Penas, which has been interpreted as a pull-apart basin, and (2) the Liquiñe-Ofqui fault system along which right-lateral slip is suggested [*Hervé et al.*, 1979]. Three-dimensional finite element models [*Nelson et al.*, 1994] of the Chile ridge subduction setting substantiate development of an arc-parallel fault at about 150-200 km from the trench. The Liquiñe-Ofqui fault system is interpreted as a complex zone of strike-slip faulting that coincides with the forearc-arc boundary and bounds the eastern margin of the Chiloe block considered as a terrane.

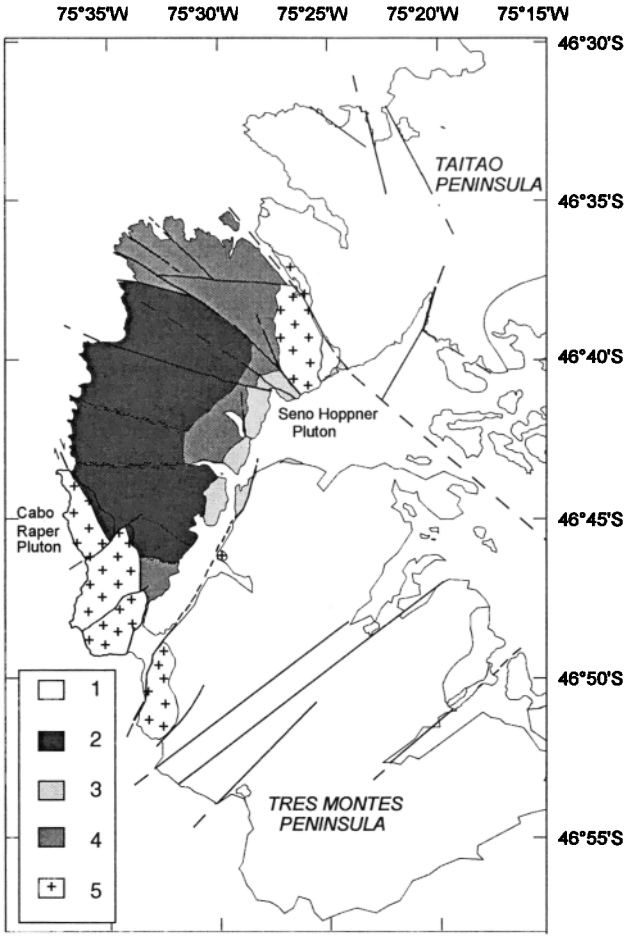

Figure 3. Simplified geologic map of the Taitao peninsula after *Mpodozis et al.* [1985], *Forsythe et al.* [1986], and *Bourgois et al.* [1996]. Units are as follow: 1, pre-Jurassic metamorphic basement; 2, Bahia Barrientos ophiolite; 3, Chile margin unit; 4, main volcanic unit; 5, Pliocene plutons.

The Taitao and Tres Montes peninsulas located 50 to 110 km south of the Chile triple junction form the westernmost promontory of the Chile coast. Volcanic and plutonic rocks of Pliocene age exposed along this promontory are located at <17 km landward from the trench axis. Conversely, these rocks are buried under a thick accumulation of slope sediment in 1000 to 3000 m deep water, to the north and to the south of the promontory. The Taitao and Tres Montes peninsulas are a window on the geology of the lower and midslopes of the Chile continental margin. Five main tectonic units (Figure 3) are recognized in the Taitao and Tres Montes peninsula area [*Mpodozis et al.*, 1985; *Forsythe et al.*, 1986; *Kaeding et al.*, 1990; *Bourgois et al.*, 1993, 1996]: (1) pre-Jurassic metamorphic basement rocks, (2) the Bahia Barrientos ophiolite, (3) the volcanic-sedimentary Chile margin unit, (4) the main volcanic unit which correlates with the Chile margin unit, and (5) the plutonic suite which includes the Cabo Raper and Seno Hoppner plutons. The Chile margin unit [*Bourgois et al.*, 1993] consists of interbedded sedimentary and volcanic material. Its estimated thickness is 4-6 km. The base of the sequence unconformably overlies the pre-Jurassic metamorphic basement of the Chile margin. Nannoplankton assemblages are

of early Pliocene age (5-5.3 Ma) at the base of the sequence and of early Pleistocene age (1.5-1.6 Ma) in strata close to the top of the sequence. A shallow water depositional environment characterized the Chile margin unit throughout. Bedding exhibits a subvertical to vertical attitude along major strike slip faults. From 5-5.3 Ma to 1.5-1.6 Ma, an area of the Chile margin located today above sea level at <40 km from the Chile trench axis was in upper slope to shelf water depth conditions and had undergone a continuous subsidence of 4-6 km. The tectonic regime, which is closely correlated to the Chile ridge and transform migration beneath the Taitao peninsula area [*Bourgois et al.*, 1996], changed abruptly from subsidence to uplift sometime later than 1.5-1.6 Ma. Of particular interest is the 4-6 Ma Cabo Raper pluton located at the seaward edge of the Taitao peninsula. Its chemical characteristics, similar to those of adakitic or trondhjemite-tonalite-dacite suites, combined with tectonic data allowed *Bourgois et al.* [1996] (1) to reconstruct the paleogeometry of the Chile margin at the time of the Cabo Raper pluton emplacement and (2) to estimate quantitatively the volume of material removed by subduction-erosion in association with the Chile ridge subduction beneath the Taitao peninsula. These results emphasized the particular role of the subducting Chile ridge as an agent that may contribute to increase the rate of subduction-erosion at depth and therefore to strongly influence the tectonic regime of the continental margin.

During ODP Leg 141, five sites (Figure 1) were drilled along the Chile continental margin. Sites 859, 860, and 861 were drilled along a transect located 10 km south of the Darwin fracture zone with the objective of providing a characterization of the continental slope 100 kyr prior to ridge collision. Site 863 is located few kilometers south of the Chile triple junction, in an area where the axis of the spreading ridge subducted at 50 ka. Finally, Site 862 was drilled along the Taitao ridge interpreted to be an igneous body that may be the seaward extension of the Bahia Barrientos ophiolite. The sediments drilled during ODP Leg 141 are Quaternary to early Pliocene, the oldest recovered sediment being 4.2-4.3 Ma in age. The lithology of rocks [*Behrmann et al.*, 1994] recovered at Sites 859, 860, 861, and 863 includes detrital sediments with grain size ranging from clay to gravel and conglomerate. By contrast to the Taitao and Tres Montes peninsula area, no volcanic rock was recovered here. Site 862 located on the crest of the Taitao ridge drilled 20 m of sediments overlying volcanic rocks. Microfossil assemblages [*Behrmann et al.*, 1992a] from the sediment indicate an age of late Pliocene, meanwhile rhyolitic samples provided Ar/Ar ages of 1.54±0.08 and 2.2±0.4 Ma [*Forsythe et al.*, 1995]. New detailed geochemical investigation on volcanic rock recovered during ODP Leg 141 [*Guivel et al.*, 1999] allowed comparison with equivalent volcanic suites exposed onland along the Taitao peninsula [*Bourgois et al.*, 1993; *Lagabrielle et al.*, 1994; *Le Moigne et al.*, 1996]. The magmatic products erupted on both structures exhibit similarities in chemical signature and age.

4. Paleoclimatic Background

Glacial events which are supposed to increase the rates of terrigenous trench sedimentation can affect not only the accreted volume [*von Huene and Scholl*, 1991] but also the tectonic regime at convergent margins. Wedge-shaped bodies of axial trench turbidite deposits were described in high-

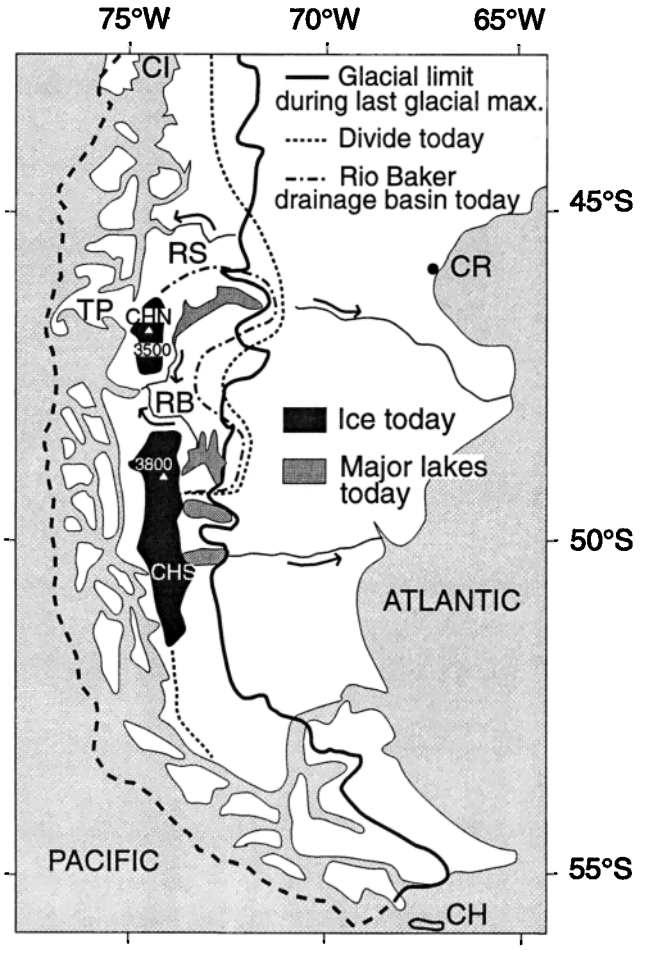

Figure 4. Limits of the last glacial maximum and distribution of existing ice field. Campo de Hielo Norte (CHN); Campo de Hielo Sur (CHS); Cabo de Horno (CH); Chiloe Island (CI); Comodoro Rivadavia (CR); Rio Baker (RB); Rio Simpson (RS); Taitao peninsula (TP). Note that the development of the ice cap during the Last Glacial Maximum prevents drainage to the Pacific as the Rio Baker acts today.

latitude trenches [*Kulm et al.*, 1973; *Scholl*, 1974]. These wedges are only a few hundred thousand years and can thus rapidly thicken the trench infill entering the subduction. Off southern Chile, *Bangs and Cande* [1997] argued that the glacial climate and climatic variations in this region caused significant fluctuation in trench sediment supply that in turn influenced the tectonic regime. The succession of short episodes of accretion, nonaccretion, and erosion observed between 35°S and 40°S is proposed to be linked to variation in trench sediment supply.

During the Last Glacial Maximum, ~20 kyr the Patagonian ice cap (Figure 4) extended 1800 km along the Andes [*Hollin and Schilling*, 1981; *Porter et al.*, 1992]. From Cap Horn at 56°S to Chiloe island at 42°S, ice totally covered the Andean reliefs from the Argentina Andean piedmont to the Pacific shoreline. The last glaciation ended with massive collapse of ice lobes close to 14 kyr ago [*Lowell et al.*, 1995]. Since that time, the ice cap retreated to its present distribution, restricted to the North and South Patagonian ice fields.

The climate of Patagonia is dominated by the Pacific Ocean to the west, the Andean Cordillera with peaks rising above

3000 m, and the dry plains of Argentina to the east. The cool temperate belt extends south of 42°S [*Miller*, 1976], with the westerlies and precipitation reaching a maximum around 50°S. Here, mean annual precipitation may exceed 5000 mm at sea level. Precipitation totals decline sharply northward from 2000 mm at 40°S to <150 mm at 30°S. Numerical modeling to reconstruct the climate of Patagonia during the Last Glacial Maximum [*Hulton et al.*, 1994] shows a northward migration of the precipitation belt of ~5° latitude with a decrease of the annual precipitation totals at 50°S, and an increase at latitude 40°S, the westerlies reaching a maximum at 45°S. The topographic barrier of the Andes is expected to influence atmospheric circulation in a similar way during both glacial and nonglacial periods.

Therefore, along the survey area transect, between 45°S and 48°S latitude, we may infer the succession of two different periods during the last glacial-interglacial cycle: (1) a glacial period with ice-rafted detrital discharge similar to the Heinrich events described in the northern Atlantic and low river output to the Pacific and (2) a warmer period during which the ice cap retreat allowed the Patagonia Andean piedmont to be drained off to the Pacific Ocean, across the Andes through the Rio Baker stream system (Figure 4). During the Last Glacial Maximum, the upper layer circulation of the southern Pacific Ocean and the westerlies had the same strong westward pattern as today. Only a modest northward migration occurred. Therefore we infer that icebergs originating from the Patagonian ice cap were permanently drifting along the Pacific South America shoreline, with Patagonian ice-rafted discharges being restricted to areas close to the Chile shoreline.

In a recent reanalysis of the $\delta^{18}O$ time series, *Winograd et al.* [1997] show that the last four interglaciations, i.e., isotopic substages 5e, 7e, 9c, and 11c, range from 20 to 26 kyr in duration. Each of these warm events was followed a cold period of about 60 to 80 kyr in duration. Therefore five glacial-interglacial cycles being 80 to 120 kyr in duration occurred during the past 500 kyr. The warmest portion of the last interglaciation, i.e., substage 5e, is marked by a $\delta^{18}O$ plateau which documents an ice volume similar to the one observed today. Moreover, the uranium series dated corals marking the last interglacial sea level high stand provide evidences that sea level was above modern levels between 130 and 117 ka. Therefore we suspect that the Patagonian ice cap may have suffered a massive retreat between 130 and 117 ka allowing the river systems, including the Rio Baker river system, to be reactivated as they are today in the Andes. It is commonly considered that the rate of delivery of terrigenous sediment increases during glaciation along high-latitude trenches [*von Huene and Scholl*, 1991]. In the specific situation of southern Chile we suspect that (1) major supply of sediment to the trench axis occurred during the short interglaciation periods since 2-3 Ma and (2) conversely, glaciation periods were characterized by low sediment supply to the trench axis and ice-rafted discharges restricted to the upslope area, close to the shoreline.

5. Presubduction Segment (45°10'-45°50'S)

The subduction front (Figure 5) is sinuous resulting from a succession of overlapping lobes protruding into the trench. One of these lobes (Figure 6) between 45°23'S and 45°32'S, along the seismic line 2, exhibits the characteristics of a slump which originated from a concave-up scar located 10-12 km landward from the subduction front. The top of the displaced block tilted landward produced a reverse slope. The estimated displacement of the block is 5 km as a minimum. Therefore the Chile margin morphology as a whole appears to be shaped by mass wasting and landslide processes. Failure of oversteepened slopes is indicative of continental margin subsidence sustaining slope instability. Similar features are observed frequently along margins undergoing active subsidence, considered commonly as the typical signature of subduction-erosion at depth [*Scholl et al.*, 1980; *von Huene and Scholl*, 1991]. Therefore we may assume that massive slumping and mass wasting documented between 45°10'S and 45°50'S, reflect active subduction-erosion at depth. This tectonic regime is consistent with the narrowness of the continental slope along this segment of the Chile continental margin.

Four seismic lines (lines 1 to 4, Figures 2 and 5) were recorded along the presubduction segment. Line 3 (Figure 7) shows the main stratigraphic and morphotectonic elements of this area, including the downgoing Nazca plate, the trench axis and the lower continental slope. Along this section of the Chile trench located between the Darwin and Guamblin fracture zones, the trench fill exhibits two depositional sequences. A 700-m-thick accumulation of well acoustically stratified sediment overlies a more transparent seismic facies and some poorly defined parallel configurations. The lower transparent layer is ~100 m thick. The horizontally stratified trench infill exhibits a total thickness increasing considerably landward. It clearly onlaps the Nazca plate sedimentary cover. This demonstrates that landward tilting of the volcanic basement occurred before the trench sediment accumulated as imaged along line 3 (Figure 7). Along line 3 the flat floor of the Chile trench axis is ~19.2 km wide. Because the convergence rate between Nazca and Antarctica plates is about ~8 cm/yr, subduction of the sediment accumulation, as shown along line 3 today, will take <250 kyr. As a consequence, we assume that line 3 exhibits trench sediment not older than 250 ka. Therefore roughly 700 m of trench fill sediment accumulated in <250 kyr, at a rate of 2800 m/Myr that is twice as much the 1500 m/Myr rate documented in the gulf of Alaska at deep sea drilling Site 180 [*Kulm et al.*, 1973]. The trench fill increases in thickness to the north, from 700 m along line 3 to 1100 m north of the Guamblin fracture zone, along line 1 (not shown). By contrast, the Chile ridge axial valley located in the southward extension of the Chile trench is nearly devoid of sediment. Active trench sedimentation in the surveyed area is controlled by the Chile ridge subduction that appears to be damming the trench sediment supply originating from the north [*Bangs and Cande*, 1997].

Along line 3, two reverse faults with <10 m offset are observed at 1.5 and 3 km seaward of the subduction front, respectively. These high-dipping landward faults which crosscutt the trench sediment upper sequence root at depth in the lower transparent layer. Similar tectonic elements exist on both lines 3 and 1, meanwhile lines 2 and 4 show trench sediment accumulation devoid of tectonic disruption. However, we assume that the two faults imaged along lines 1 and 3 in the trench infill also exist along line 2 but are covered by the above described slump. Since the trench sediment accumulation shows little disruption and tectonism, we attribute the trench infill to rapid influx of sediment. The ~1.5 km spacing of reverse faults imaged along lines 1 and 3

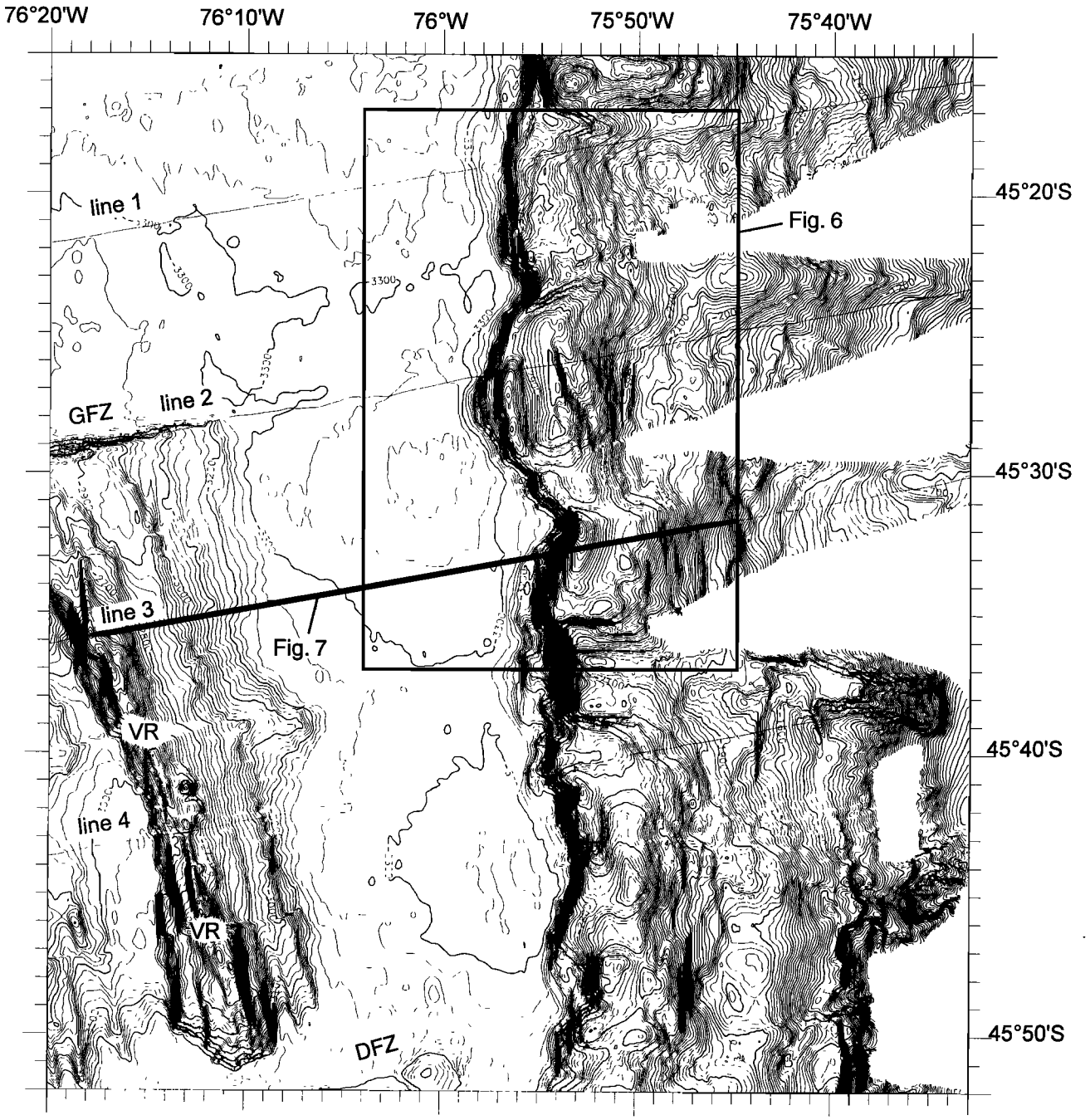

Figure 5. Bathymetric map (contours are every 20 m) of the Chile trench and continental margin along the presubduction segment. Locations of Figures 6 and 7 are shown. Darwin fracture zone (DFZ); Guamblin fracture zone (GFZ); volcanic ridge (VR). Location is shown on Plate 1.

documents that accretion is currently active along the trench axis. Nearly all of the 700 m of trench sediment is accreted to the continental margin in two separated sheets. The ~10 m upward displacement of the horizontally stratified sediment of the hanging wall shows no significant variation with depth indicating that fault propagation occurred recently, after the trench sequence accumulated.

6. Synsubduction Segment (45°50'-47°10'S)

The Chile ridge subsegment (Figures 8a and 8b), which extends from 45°50'S to 46°09'S over a distance of 35 km from the Darwin fracture zone to the north to the Chile triple junction to the south, is characterized by a prominent scarp at the toe of the continental margin. This 250 to 750 m high scarp (Figure 8a) allows us to easily identify the subduction front. The acoustic imagery (Figure 9) and the analysis of bathymetry allow to accurately locate the Chile triple junction. The subduction of the Chile ridge spreading center occurs at 46°09'S, in an area close to a volcanic edifice which has been sampled by dredging during the CTJ cruise. This volcano protruding within the CRS 1 axial valley is currently underthrusting below the Chile continental margin or venting through the toe of the continental wedge.

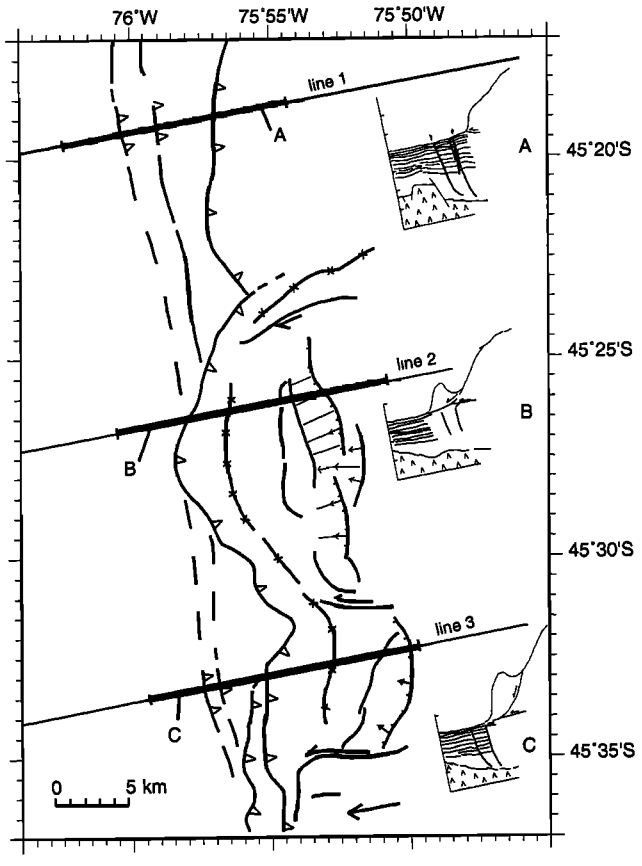

Figure 6. Structural sketch of an area of the presubduction segment. Line with tick marks shows normal fault, line with open triangles shows thrust fault including the major decollement at the subduction front, and line with crosses shows anticline dome axes. A, B, and C indicate line drawing of profiles (thick line). Reverse faults imaged along profiles A (seismic line 1) and C (seismic line 3) are supposed to exist (dash line) along profile B (seismic line 2) beneath a slump lobe protruding into the trench. See text for more details. Location is shown on Figure 5.

The axial valley of the CRS 1 (Figure 9), characterized by high-reflectivity terranes, is an active spreading center. The average width of the active domain is 3 to 6-7 km and corresponds to a deep elongated graben devoid of significant sediment accumulation. The trench axis on lines 6 (not shown) and 7 (Figure 10), which lies 5 and 3 km east from the axis of the spreading ridge, respectively, is also relatively free of sediment as it is just north along line 745 [*Bangs et al.*, 1992]. This situation is all the more remarkable because the Chile ridge axial graben and the CRS 1 connect northward to the Chile trench axis where sediment infill is hundreds of meters thick. South of the Chile triple junction, the Chile trench axis, which connects to the North Taitao canyon at 46°21'S, is in the exact southward prolongation of the Chile ridge axial valley. Because a N90-120°E trending ridge (Figures 8a and 8b) obstructs the Chile trench axis at 46°23'S, the detrital material bypassing through the North Taitao canyon has to be carried to the north along the Chile trench axis and the Chile ridge axial valley. Since these two morphological deeps show no significant accumulation of sediment, we assume that little detrital material transits through the North Taitao canyon today.

The CRS 1 shows (Figure 10) a bathymetric transverse section asymmetric with a landward rift valley wall lying ~100-150 m deeper than its seaward conjugate flank reflecting the accumulated overburden of the lower continental slope as entering the subduction [*Bangs et al.*, 1992]. Conversely, the seaward rift valley wall is a prominent relief with rectilinear normal fault scarps offsetting the ridge flanks. This relief bounds a domain with 55 to 120 m thick sedimentary cover west of the Chile ridge active domain which is devoid of sediment. The fabric of the ocean crust that extends 20-25 km west of the rift valley is dominated by seaward tilted blocks (Figure 10). Sediments accumulated in the half graben structures exhibit fan-shaped turbidite accumulation onlapping older tilted blocks. This area of the Antarctic plate appears to have been the locus of polyphased extensional tectonics. At least two pulses can be recognized in this area close to the active spreading axis.

The tectonic history of the continental margin along the Chile ridge subsegment is well constrained by ODP drilling data acquired at Sites 859-861 located on multichannel seismic line 759 (Figure 8b). According to *Behrmann et al.* [1994], subduction-accretion ceased during the late Pliocene after an important phase of forearc building which occurred in the early to late Pliocene. During the past ~2 Myr, sediments of the downgoing oceanic plate have been subducted. The subduction-erosion inferred at depth is consistent with not only the tectonic evolution [*Bangs et al.*, 1992] of the seawardmost basin sediment and normal faults identified along line 745 (Figure 8b) but also the tectonic regime of the continental margin to the north.

The North Taitao canyon subsegment extends from 46°09'S to 46°26'S (Plate 1). As to the north, a 100 to 150 m high scarp with high backscatter in the acoustic EM12 imagery (Figure 9) allows us to define clearly the subduction front, also crosscutting the mouth area of the North Taitao canyon. At 46°12'S, the high-reflectivity terrane of the CRS 1 to the north and the thick sediment accumulation which characterizes the Chile trench to the south exhibit a sharp contact in the EM12 acoustic imagery (Figure 9). Indeed, line 9 (Figure 11), which lies close to line 751 (Figure 8b) described by *Bangs et al.* [1992], exhibits a trench fill with a considerably greater thickness than to the north. This trench fill is bounded seaward by a set of parallel normal faults which offsets the top of the oceanic crust by ~500 m downward. The trench fill thickens southward exhibiting a ~500 m maximum thickness accumulation along line 10, at the mouth area of the North Taitao canyon. To the west, the sediment accumulation is 100-180 m thick. As in the north, this sediment cover recorded a tectonic evolution through two extensional pulses. However, the fault system here trends ~N0°, making an angle of ~20° with the average direction of faults bounding the CRS 1. Structures along line 10 (Figure 12) are more complex than to the north along line 9. They include compressional tectonic features along the trench axis associated with the N90-120°E trending ridge uplifted along a reverse fault at 46°23'S (Figures 8a and 8b). This 100-120 m high ridge is associated landward with minor ridges which outline morphologically thrust sheets displaying an imbricate stack at depth similar to a flower structure (Figure 12). The reverse faults at the thrust sheet boundaries root at depth along a major normal fault belonging to a set of normal faults which marks the seaward wall of the trench axis at depth. This indicates that tectonic inversion occurred along one of these faults, at least.

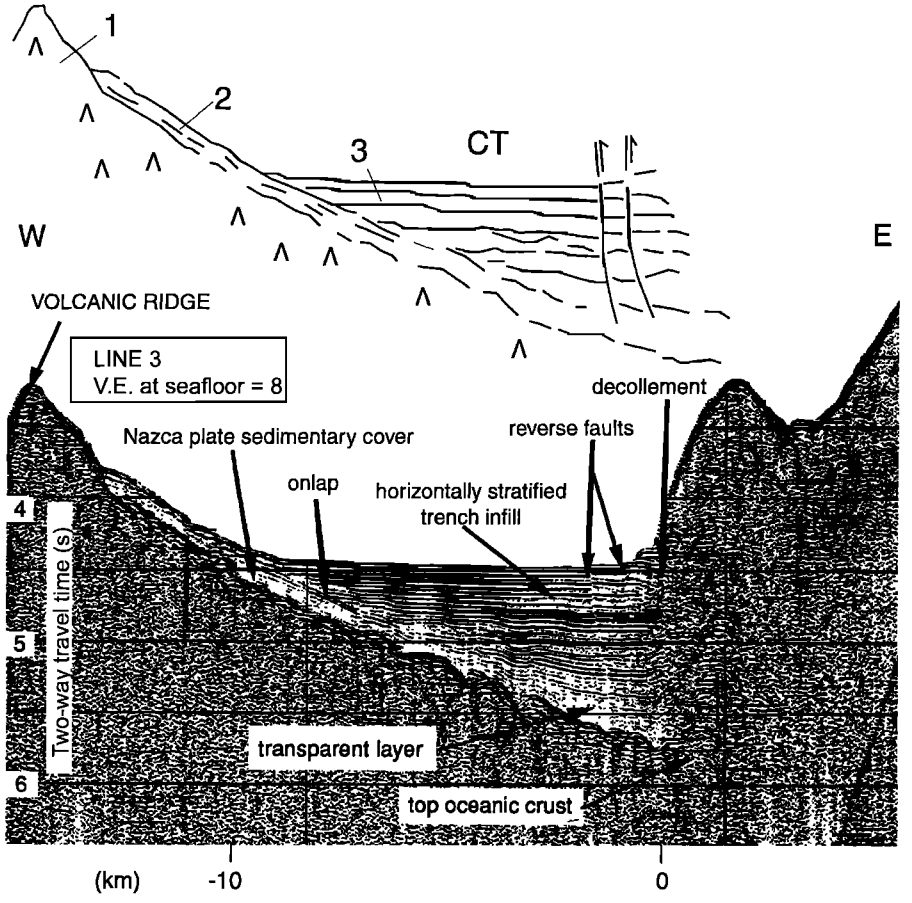

Figure 7. Trench section of the seismic line 3. Horizontal scale marks distance from the subduction front in kilometers. Note the reverse faults in the trench fill associated with incipient accretion. See text for more details. Line drawing inset shows Chile trench (CT); 1, oceanic crust; 2, Nazca plate sedimentary cover; 3, trench infill. Location is shown on Figure 5.

The deformation front along the North Taitao Canyon subsegment (Figures 8a and 8b) has a sigmoidal shape with a left lateral offset of 2 km along the compressional ridges of the Chile trench at 46°23'S. The EM12 imagery data (Figure 9) show a clear connection between the main reverse fault bounding these ridges to the south and the left-lateral strike-slip fault offsetting the decollement landward. This is in good agreement with the flower structure imaged along line 10 (Figure 12). Along the continental margin this transpressional fault system bounds a prominent E-W trending ridge forming to the north the southern wall of the North Taitao canyon.

North of the North Taitao canyon, the EM12 bathymetric map displays three main morphotectonic features. From west to east (Figure 8b) it includes the frontal ridge along the main decollement, a wide dome-shaped relief (i.e., the middle slope dome (MSD, Figure 8b)) and a major scarp (i.e., the upper scarp hereafter (US, Figure 8b)) with surface slope steepness of ~12°, dipping twice much as to the north. Along seismic line 751 [*Bangs et al.*, 1992], the frontal ridge appears to be pushed up at the base of the trench slope. About 6-8 km toward the trench on the lower slope is a 600-700 m high scarp along the seaward edge of the MSD which exhibits a strong asymmetry in section with a peculiar flat plateau below the US. The US at the upper middle slope boundary exhibits two different segments. The northern segment (NS, Figure 8b) is in the southern extension of the Chile ridge spreading center and trends subparallel to it. The southern segment (SS, Figure 8b), which trends nearly perpendicular to the northern segment, parallels a slightly bent ridge located along the northern rim of the North Taitao canyon. The morphology considered as a whole, including the MSD and the two US segments (NS and SS) that both exhibit a seaward concave shape and a decrease in height to the north and to the south, is typical of a slump. The MSD resulted from a slope failure along a concave-up slip surface from which the US scar originated. The top of the dome tilted backward resulting in the quasi-reverse flat surface at the top of the MSD; meanwhile, the hummocky disorganized topography at the toe of the seaward slope protruded into the trench floor and was subsequently uplifted along the subduction front. Small irregular-shaped mounds dot the uplifted flat trench floor between the subduction front and the seaward slope of the dome-shaped relief. The morphological protrusion and the isolated mounds on the flat uplifted trench floor indicate a debris flow in the trench axis with isolated outrider blocks. However, since the US shows no clear signature at depth in seismic line 751, we assume that these morphological characteristics are those of a detachment fault dipping seaward, as previously proposed by *Bangs et al.*

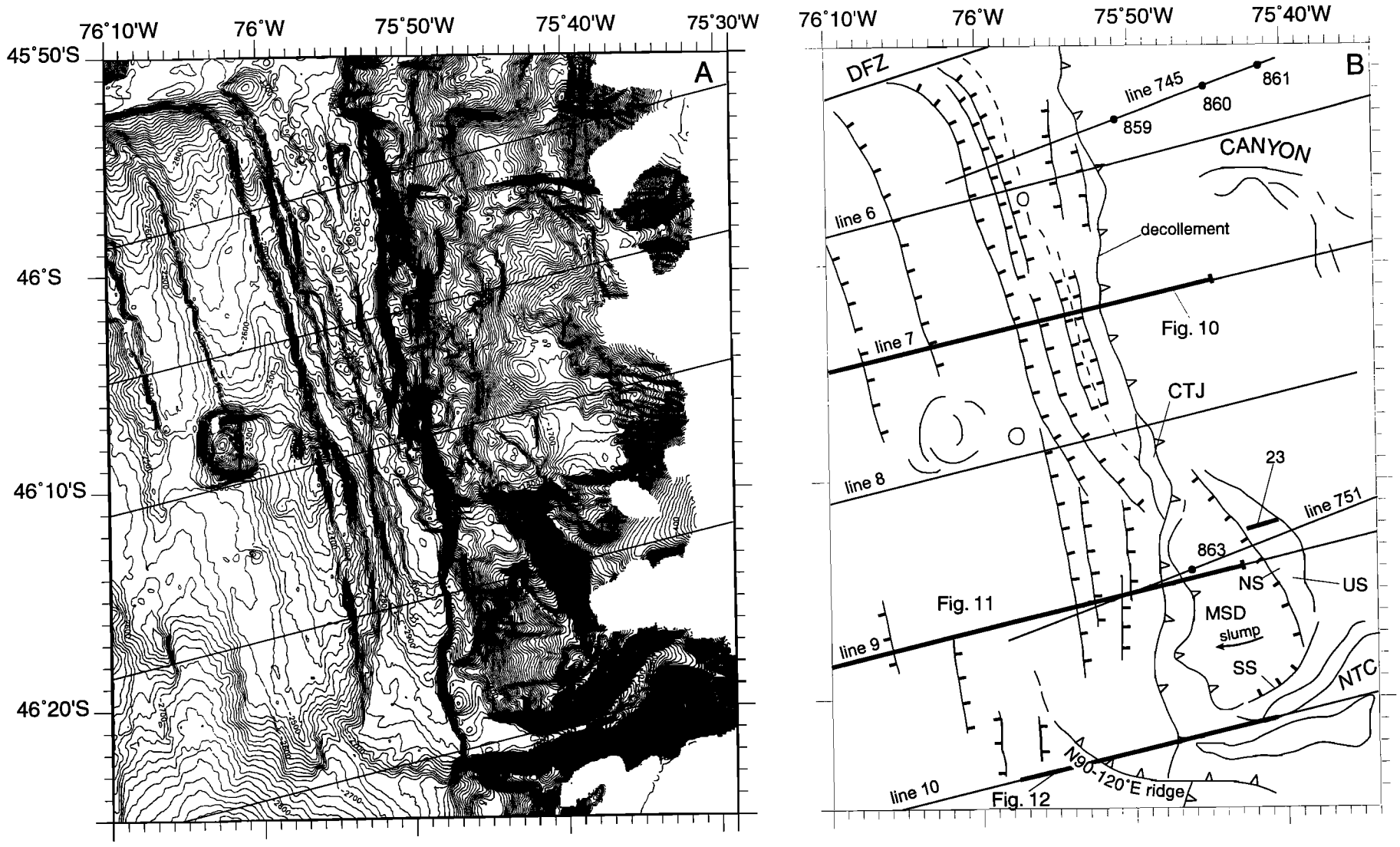

Figure 8. The Chile ridge subsegment. (a) Bathymetric map (contours are every 20 m). (b) Structural sketch of the area shown in Figure 8a. Line with tick marks shows normal fault, line with open triangles shows thrust fault including the major decollement at the subduction front, dashed line shows the axis of the CRS 1, and solid dots with numbers mark ODP Leg 141 sites. Locations of Figures 10, 11, and 12 are shown. Chile triple junction (CTJ); dredge site (23 and the thick short line); Darwin fracture zone (DFZ); middle slope dome (MSD); northern scarp (NS); North Taitao canyon (NTC); southern scarp (SS); upper slope scarp (US). Location is shown on Plate 1.

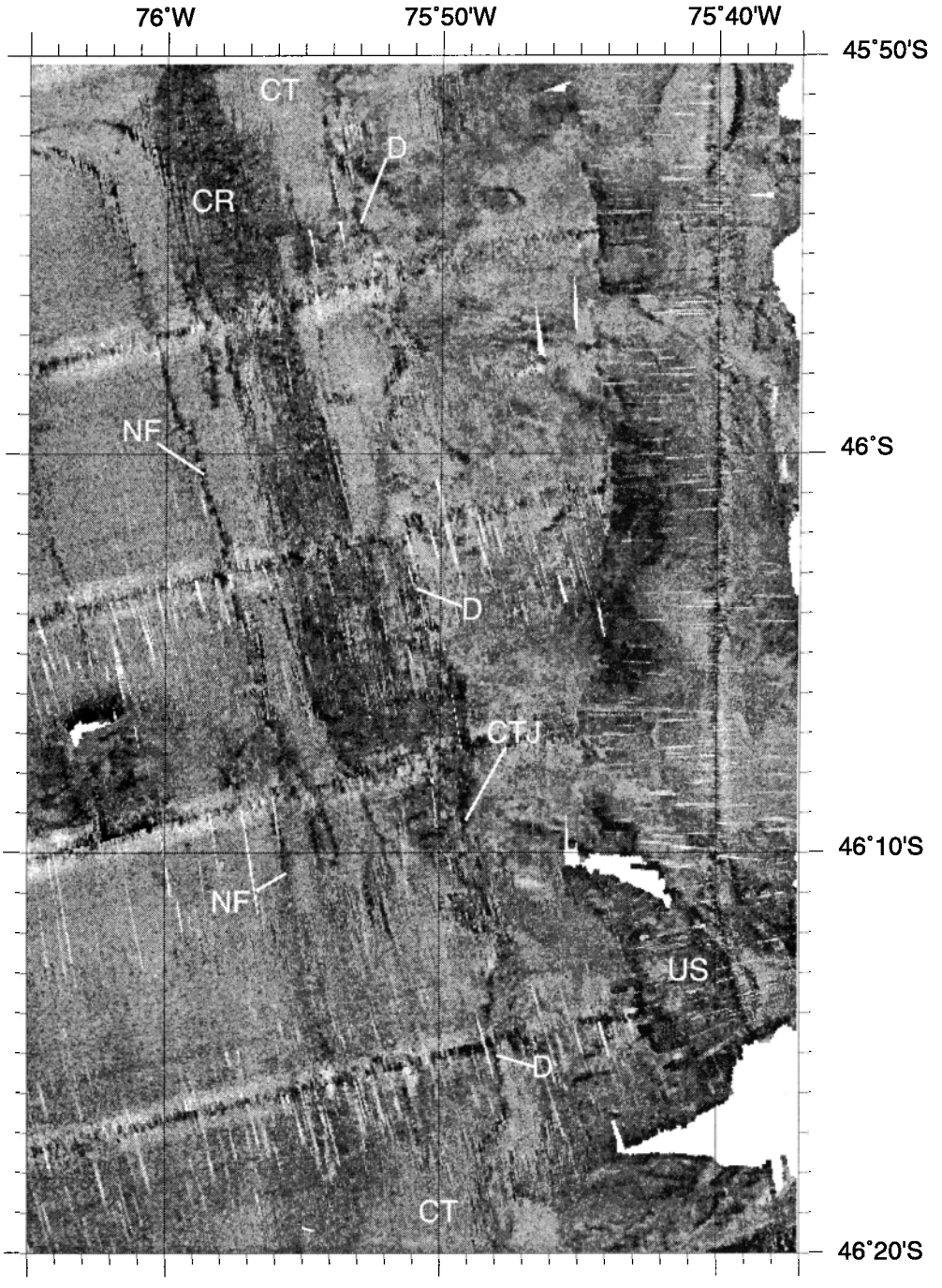

Figure 9. EM12 imagery of the Chile ridge subsegment. Note the high backscatter of the axial valley of the CRS 1. Chile ridge (CR); Chile trench (CT); Chile triple junction (CTJ); decollement (D); normal fault (NF); upper slope scarp (US). See text for more details. Location is shown on Plate 1.

[1992] and *Behrmann et al.* [1994]. As a consequence, they speculate that outcrop of the continental margin metamorphic basement should exist along the upper scarp. This assumption was verified during the CTJ cruise. Dredging (CTJ 23, Figure 8b) along the US allowed us to recover metamorphic rocks similar to the pre-Jurassic continental basement of the Tres Montes and Taitao peninsulas (Figure 3).

The E-W trending middle course of the transverse North Taitao canyon (Figure 13a) is 1250-2000 m deep. This prominent morphological feature opens a window into deep structures of the Chile continental margin. It exhibits an asymmetrical transverse cross section. The southern wall of the canyon is 750-1250 m higher than its northern wall, suggesting that subsidence occurred to the north. Five dredges (Figures 13a and 13b) have been performed along the canyon walls. Two dredges (42 and 44, Figure 13b) located along the southern wall at 10 and 15 km landward from the trench axis recovered pre-Jurassic metamorphic rocks similar to those sampled onland [*Mpodozis et al.*, 1985; *Forsythe et al.*, 1986; *Bourgois et al.*, 1993] in the Taitao and Tres Montes

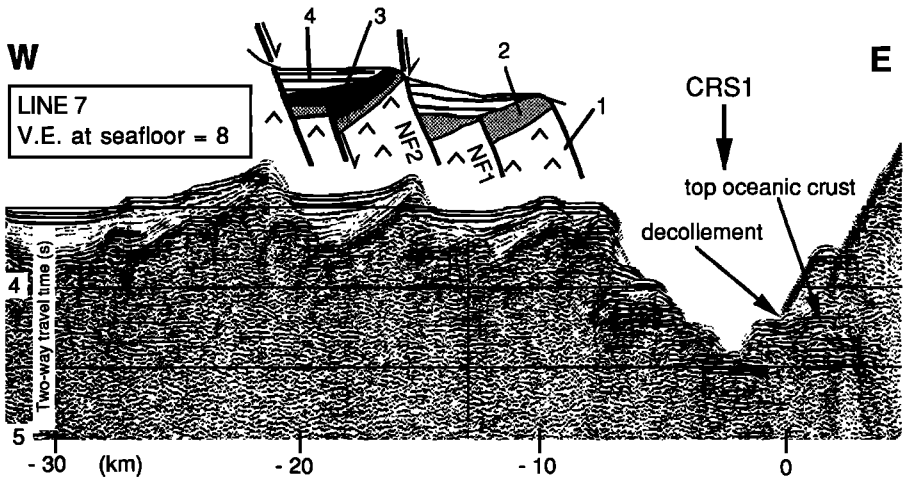

Figure 10. CRS 1 and adjacent seafloor sections along seismic line 7. Horizontal scale marks the distance from the decollement in kilometers. Note that the landward rift valley wall is deeper than the seaward wall. The tilted blocks west of the Chile ridge evolved through two tectonic pulses (NF1, normal fault of the first extensional pulse, and NF2, normal fault of the second extensional pulse). Line drawing inset: 1, oceanic crust; 2, sedimentary cover of the oceanic crust; 3, old turbidites (syn-NF1); 4, young turbidites (syn-NF2). See text for more details. Location is shown on Figure 8b.

peninsulas (Figure 3). Two other dredges (19 and 43, Figure 13b) located along the northern wall of the canyon at the same distances from the trench axis have recovered volcanic rocks and sediments having affinities with rocks of the Pliocene suites of the Chile Margin Unit and the Main Volcanic Unit described onland in the Taitao peninsula [*Bourgois et al.*, 1992, 1993; *Guivel et al.*, 1999]. This is in good agreement with subsidence of the northern wall of the canyon with respect to the southern wall. We therefore assume that a northward dipping major fault with a normal dip-slip component of ~1 km as a minimum follows the canyon course. A dredge (17, Figure 13b) located only 5 km landward from the trench axis, along the southern wall of the North Taitao canyon, recovered volcanic rocks and sediments [*Guivel et al.*, 1999] similar to those sampled along the northern wall of the canyon. The sediments which unconformably overly the Chile continental margin basement extend to within <5 km landward from the trench axis. Because the North Taitao canyon fault shows no offset of the subduction front along its westward prolongation, it must have no significant tectonic activity today.

The Taitao ridge subsegment located off the Taitao and Tres Montes peninsulas extends from 46°26'S to 47°10'S. It includes the prominent Taitao ridge (Figure 13a) regarded as a fragment of oceanic crust in the process of emplacement [*Leslie*, 1986]. Seismic data along line 762 (Figure 13b) reveal that the

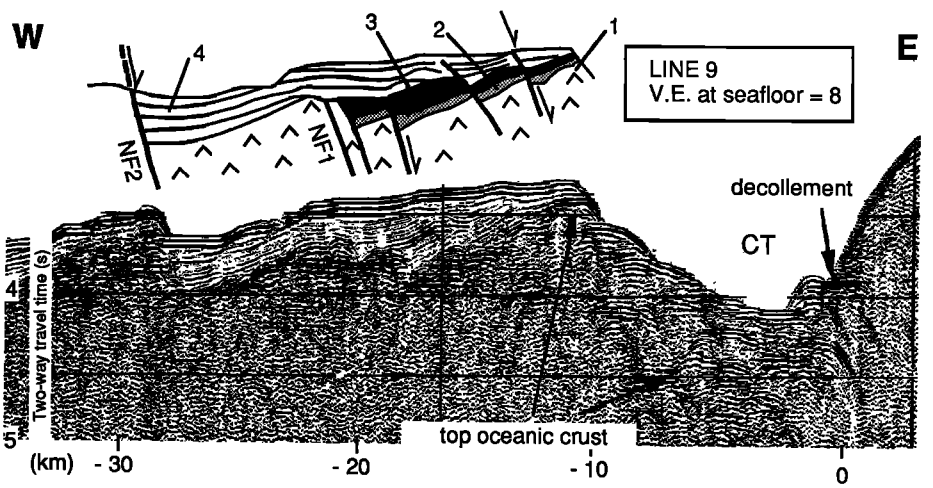

Figure 11. Chile trench (CT) and adjacent seafloor sections along seismic line 9. Horizontal scale marks the distance from the decollement in kilometers. Note the highly deformed thick accumulation of sediment along the trench axis. The tilted blocks west of the Chile ridge evolved through two tectonic pulses (NF1, normal fault of the first extensional pulse, and NF2, normal fault of the second extensional pulse). Line drawing inset: 1, oceanic crust; 2, sedimentary cover of the oceanic crust; 3, old turbidites (syn-NF1); 4, young turbidites (syn-NF2). See text for more details. Location is shown on Figure 8b.

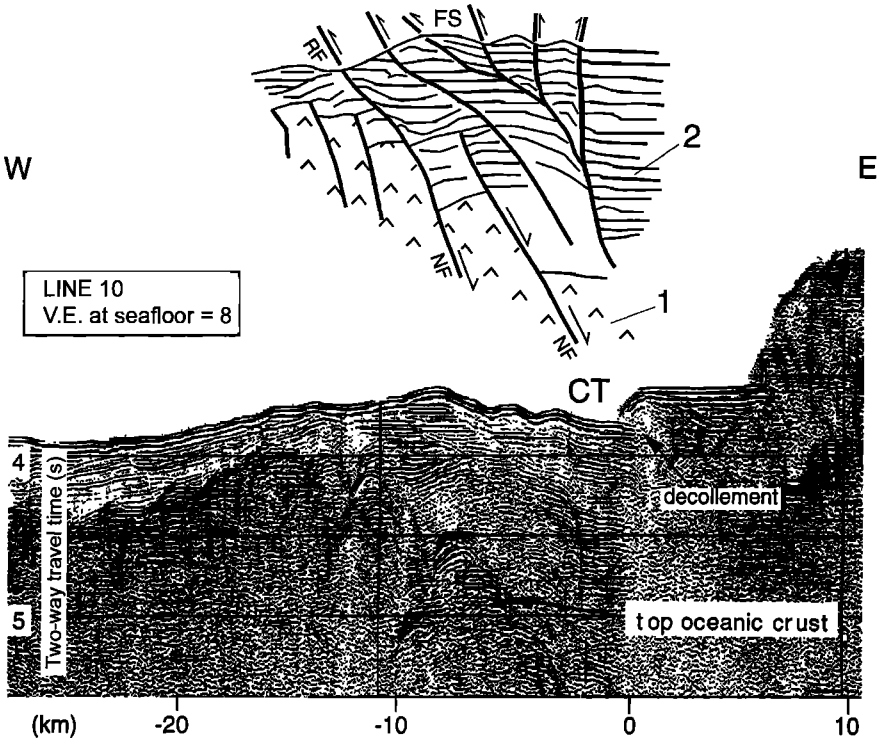

Figure 12. Chile trench (CT) and adjacent seafloor sections along seismic line 10. Horizontal scale marks the distance from the decollement in kilometers. Note the thick accumulation of sediment along the trench axis. The set of active reverse faults (thick line) exhibits the characteristics of a flower structure participating in the accumulation of thrust sheets resulting in the construction of a 100-120 m high ridge which obstructs the trench (see Figure 8). The oceanic crust is down offset along major normal faults (thin line). Inversion tectonic occurred along one of these fault, at least. Line drawing inset: flower structure (FS); normal fault (NF); reverse fault (RF); 1, oceanic crust; 2, trench infill and sedimentary cover of the oceanic crust. See text for more details. Location is shown on Figure 8b.

oceanic crust west of the section is covered by at least 700 m of sediments. To the east, the Taitao Ridge appears to represent a major tectonic slice of oceanic crust that may be the seaward extension of the Bahia Barrientos ophiolite [*Bangs et al.*, 1992]. According to *Behrmann et al.* [1994] the volcanic pile drilled at ODP Site 862 (Figure 13b) at <14 km seaward from Bahia San Andres was probably formed at a ridge-transform intersection and represents a possible candidate to become an ophiolite body emplaced into the South American forearc.

The North Taitao Ridge fault (NTRF, Figure 13b) bounding the Taitao Ridge to the north trends N55°E. Because it is rectilinear in the bathymetric map, the North Taitao Ridge fault must have a subvertical attitude. This major fault exhibits a scarp with decreasing offset to the east and finally no clear morphological signature along the Chile continental margin. Conversely, it connects seaward to an E-W trending flexure (Plate 1) that is a conspicuous feature of the Antarctica plate extending at distances as far as 100 km to the west, at least. North of the North Taitao Ridge fault, line 11 (Figure 14) shows that the oceanic crust is covered by sediments 400-450 m thick. Instead of dipping landward beneath the Taitao Ridge as see along line 762 [*Bangs et al.*, 1992], here the top of oceanic crust can be seen to tilt seaward as it approaches the ridge. These two different tectonic responses of the oceanic crust along the North Taitao Ridge fault suggest that strike-slip movement occurred along it. The along-strike bathymetry of the Antarctic plate at the toe of the North Taitao Ridge fault is characterized by a gentle slope dipping steadily to the west, from 2500 to 3250 m depth. As the Antarctic seafloor deepens to the west, the fault scarp increases in height along strike, from no significant topographic signature at point X (Figure 13b) to the east to >1200 m at point Y.

The EM12 map (Figure 13a) strongly suggests that the Taitao Ridge consists of accreted tectonic slices marked in the morphological data by two ridges (R1 and R2, Figure 13b). The R1 and R2 ridges which trend N145°E, are 7.5 and 18 km long, respectively, and exhibit a smooth morphological signature. They can be interpreted as two thrust sheets of trench sediment stacked at the toe of the main scarp (MS, Figure 13a) of the Taitao Ridge. Because it exhibits a lobe shape in map view and closely follows the 3500-m isobath, the frontal decollement must have a subhorizontal attitude at depth, at least beneath the two frontal thrust sheets, i.e., R1 and R2, Figure 13b. Along line 12 (Figure 15), the top of the oceanic crust can be seen dipping landward, suggesting that the oceanic crust is underthrusted under the Taitao Ridge. In this area, active trench floor deformation including a reverse fault at 3 km seaward from the subduction front strongly supports that subduction is active beneath the Taitao Ridge. This high-dipping landward fault, which roots at depth in a acoustically "transparent layer" (called unit T in section 7), is part of a fold and thrust belt developing seaward. Because the

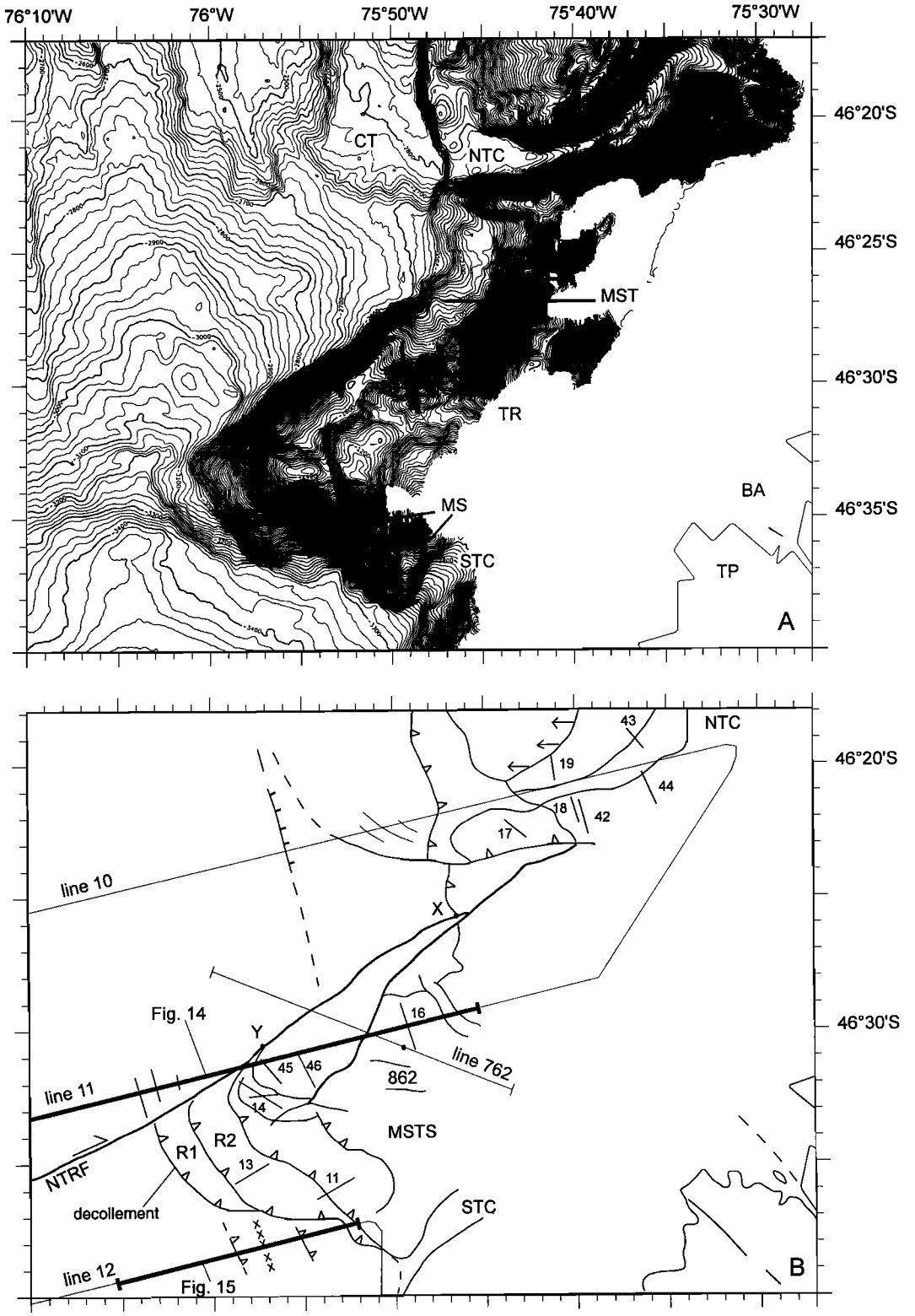

Figure 13. The Taitao Ridge subsegment along the synsubduction segment. (a) Bathymetric map (contours are every 20 m). (b) Structural sketch of the area shown in Figure 13a. Note that the structural sketch includes EM12 imagery data shown in Figure 16. Line with tick marks shows normal fault; line with open triangles shows thrust fault including the major decollement at the subduction front; solid dot marks the ODP Site 862. Locations of Figures 14 and 15 are shown. Bahia San Andres (BSA); Chile trench (CT); main scarp (MS); middle slope terrace (MST); main scarp thrust sheet (MSTS); North Taitao canyon (NTC); North Taitao Ridge fault (NTRF); ridge 1 (R1); ridge 2 (R2); South Taitao canyon (STC); Taitao peninsula (TP); Taitao ridge (TR). Dredge sites (11, 13, 14, 16, 17, 18, 19, 42, 43, 44, 45, 46, and the thick short lines in Figure 13a). Letters X and Y refer to descriptions in the text. See text for more details. Location is shown on Plate 1.

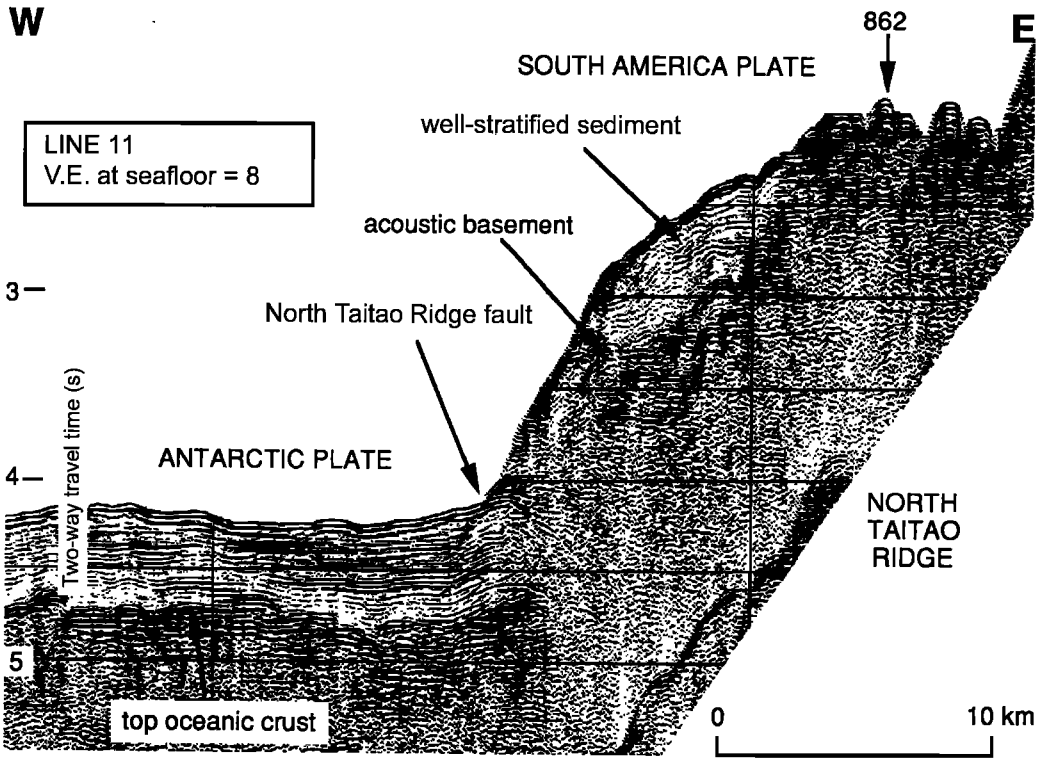

Figure 14. The Taitao Ridge and the adjacent seafloor along seismic line 11. Note that a well-stratified sedimentary cover overlies the Taitao ridge basement. Site 862, ODP site drilled during Leg 141. See text for more details. Location is shown on Figure 13b.

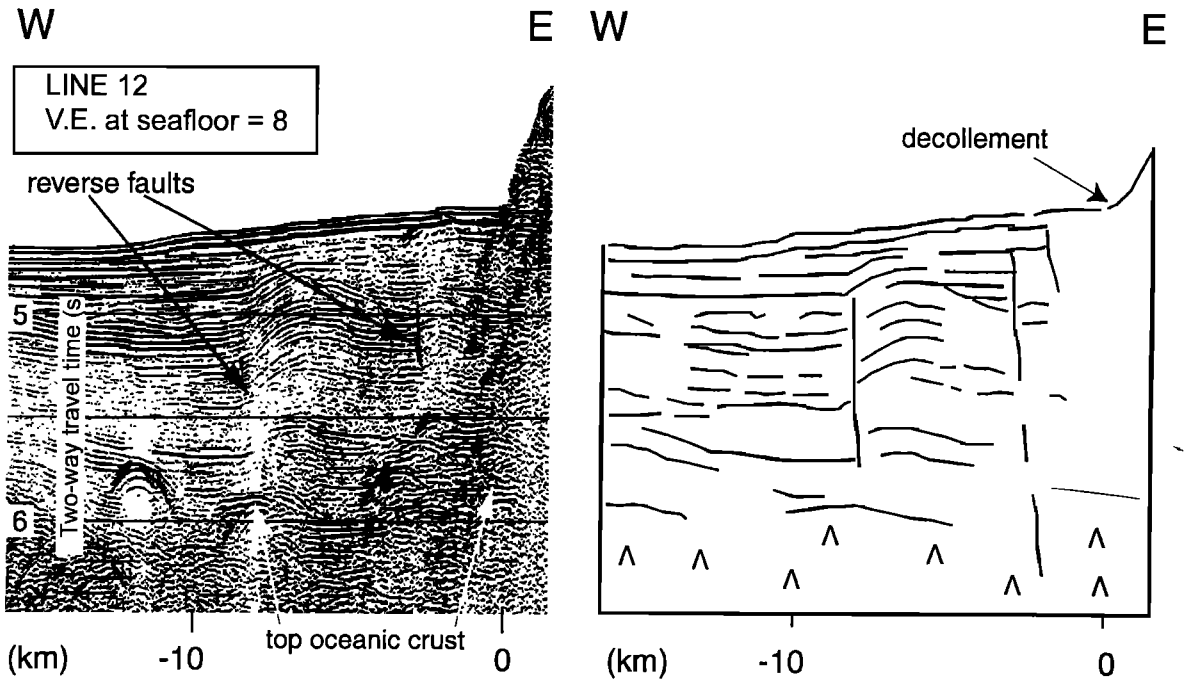

Figure 15. Chile trench along (left) seismic line 12 and (right) line drawing showing the oceanic crust and the trench infill actively underthrusted beneath the Taitao Ridge. Horizontal scale marks the distance from the decollement in kilometers. See text for more details. Location is shown on Figure 13b.

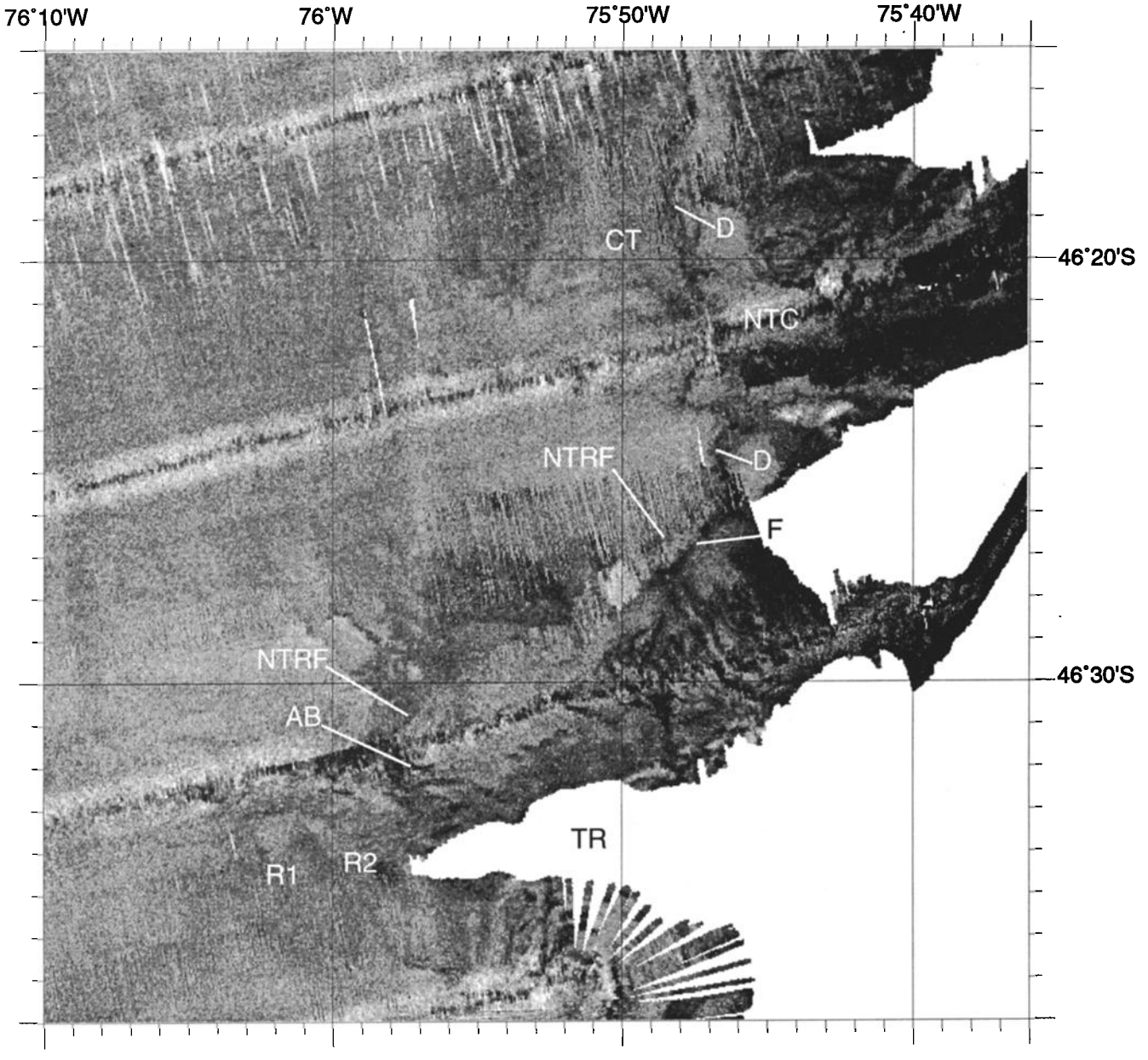

Figure 16. EM12 imagery of the Taitao Ridge subsegment. Note the low reflectivity of most of the area covered by the Taitao Ridge, including the scarp along the North Taitao Ridge fault. Acoustic basement of volcanic origin (AB); Chile trench (CT); decollement (D), fault (F); North Taitao canyon (NTC); North Taitao Ridge fault (NTRF); ridge 1 (R1); ridge 2 (R2); Taitao Ridge (TR). See text and Figure 13 for more details. Location is shown on Plate 1.

seaward thrust sheet shows no disruption and tectonism at the trench floor, we assume that the thrust sheet belt developed in two phases separated by a rapid influx of sediment in the trench. Instead, the trench fault and thrust belt are in the southeastward prolongation of the Taitao Ridge frontal accretionary prism (R1 and R2, Figure 13b), they do not connect with each other; the frontal decollement divides them.

A major feature imaged along line 11 (Figure 14) consists of the well-stratified pile of sediment covering the acoustic basement of the Taitao Ridge, west of ODP Site 862. In the EM12 bathymetric map (Figure 13a), this sedimentary sequence is associated with a N55°E trending midslope terrace (MST, Fig. 14A) that parallels the North Taitao Ridge fault. To the southeast the midslope terrace also parallels a scarp which bounds the acoustically structureless mound drilled during ODP Leg 141. The midslope terrace deepens landward along strike, from 1500-1750 to 2100-2300 m. In the EM12 imagery (Figure 16) the scarp along the North Taitao Ridge fault (NTRF, Figure 16) exhibits the same low-reflectivity signature as the midslope terrace, evidencing that the Taitao Ridge sediment comes into contact with the Antarctic plate sedimentary cover east of 75°56'W. Line 11 (Figure 14) shows the acoustic basement of the midslope terrace cropping out along the scarp of the North Taitao Ridge

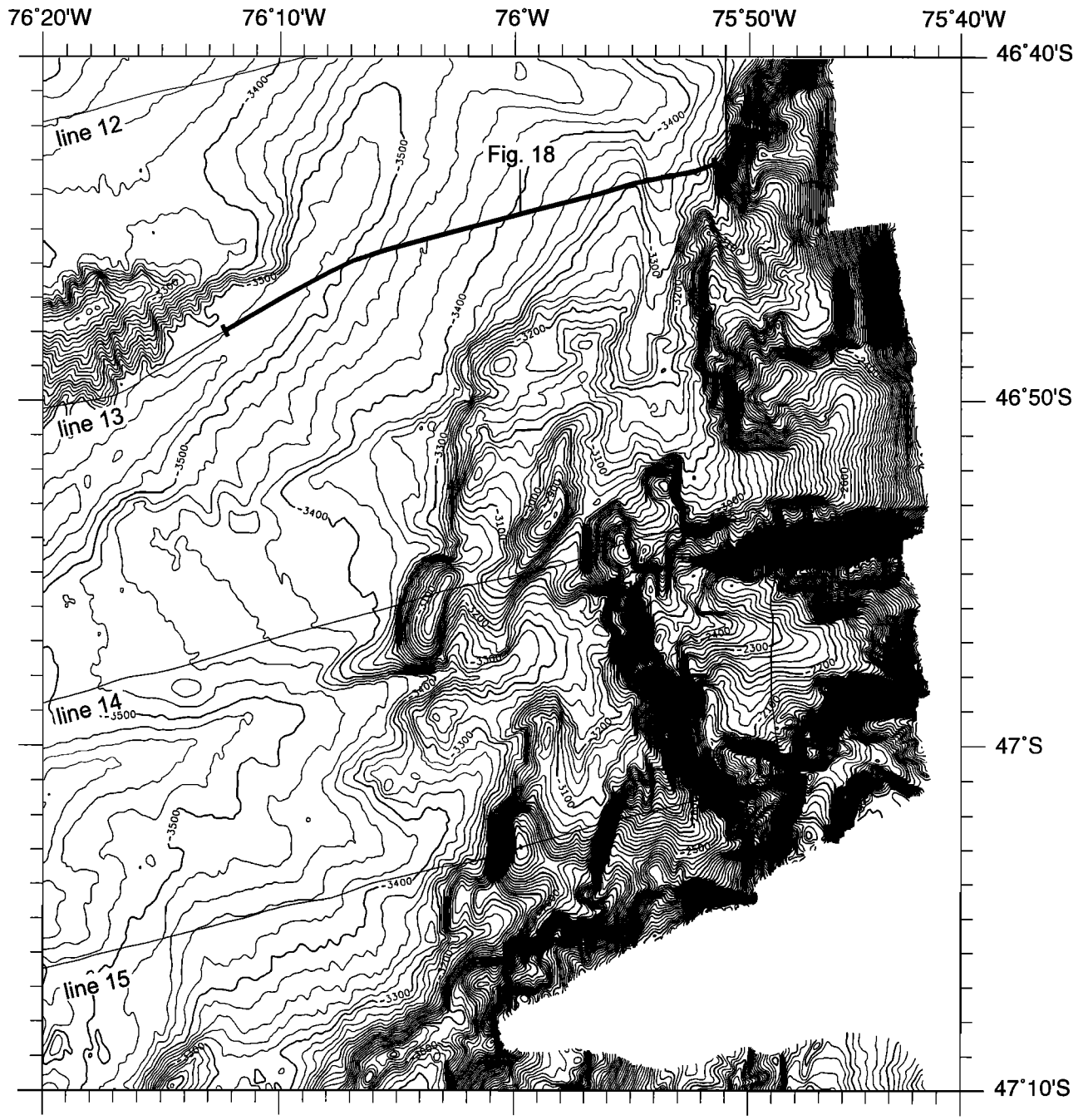

Figure 17. Bathymetric map (contours are every 20 m) of the Chile trench and continental margin along the Taitao Ridge subsegment off Taitao and Tres Montes peninsulas. Location of Figure 18 is shown. This area fits a major reentrant of the continental margin between the Taitao Ridge to the north and the Golfo de Penas accretionary prism to the south. See text for more details. Location is shown on Plate 1.

fault at 75°58'W. This acoustic basement (AB, Figure 16) exhibits a high backscatter signature in the EM12 imagery that can be followed southeastward along the main scarp (MS, Figure 13a) of the Taitao Ridge that trends parallel to the two ridges (R1 and R2, Figure 13b) of the accretionary prism west of the Taitao Ridge.

ODP Site 862 drilled a 20-m-thick sedimentary layer of Pliocene age overlying volcanic rocks of Pliocene age [*Forsythe et al.*, 1995] with chemical characteristics similar to those cropping out in the Taitao peninsula [*Guivel et al.*, 1999]. They include lavas with normal (N-type) mid-ocean ridge basalt to calc-alkaline, andesite, and dacite compositions. The volcanic basement and associated sediments drilled at Site 862 are the seaward prolongation of the volcano-sedimentary cover of the Taitao peninsula, i.e., Chile Margin unit and Main Volcanic unit (Figure 3). When associated with the EM12 acoustic and bathymetric data and seismic records along lines 11 and 762, these results suggest

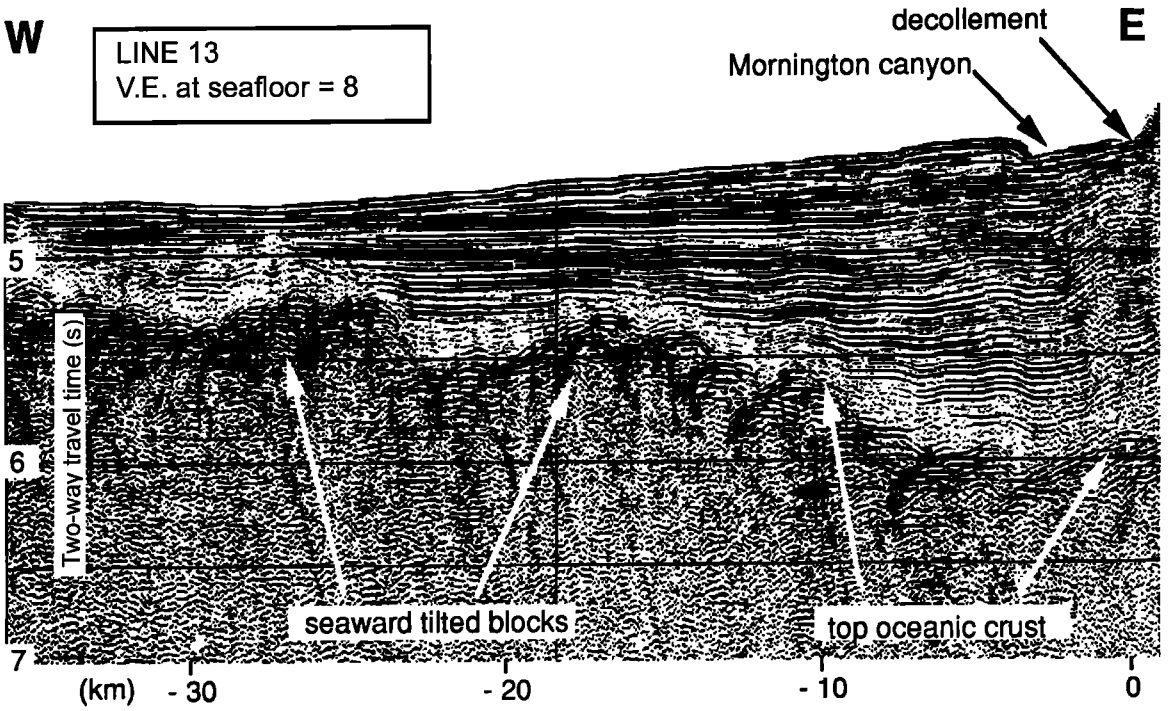

Figure 18. Chile trench along seismic line 13. Horizontal scale marks the distance from the decollement in kilometers. The trench infill onlaps two major seaward tilted blocks covered by a transparent unit. See text for more details. Location is shown on Figure 17.

that the Chile margin sedimentary cover extends seaward to the inner scarp bounding the Taitao Ridge midslope terrace. Because the midslope terrace sediments exhibit a consistent along-strike dipping attitude (55°E) and a seismic facies (Figure 14) similar to those of the adjacent Antarctic plate, we assume that the Taitao Ridge accretionary prism includes a thick midslope thrust sheet (MSTS, Figure 13b). Since dolerite and basalt were dredged along the scarp of the North Taitao Ridge fault at 75°58'W, the acoustic basement of the midslope thrust sheet imaged along line 11 is assumed to be of volcanic origin.

The section of the Chile margin south of the Taitao Ridge (Figure 17) is characterized by a major reentrant between 46°35'S and 47°10'S (Plate 1). As a consequence, at 46°50'S the Chile trench axis lies <10 km seaward of the shoreline of the Taitao peninsula. This reentrant and the associated narrow continental margin coincide with prominent morphotectonic anomalies on both seaward and landward sides including the Taitao Fracture Zone ridge (Plate 1) and the Taitao and Tres Montes peninsulas, respectively. The Taitao Fracture Zone ridge is a conspicuous E-W trending feature of the Antarctic plate. It extends west of 76°10'W throughout the surveyed area being at least 100 km long and culminates 250-300 m above the adjacent seafloor. This ridge is a southward dipping monocline bounded to the north and to the south by the Taitao and the Tres Montes fracture zones, respectively. Line 13 (Figure 18) located on the landward prolongation of the Taitao Fracture Zone ridge exhibits a 750-1000 m thick accumulation of trench sediment unconformably overlying the oceanic basement. Although the trench seafloor shows a clear seaward dip, the trench sequence exhibits a consistent quasi horizontal attitude and little tectonic deformation. By contrast, the Antarctic plate basalts beneath the trench fill are block faulted together with a thin cover of sediment. Since the trench sediment clearly onlaps these extensional deformations, we may assume that basement faulting predates the trench accumulation and therefore is not subduction-related. Finally, the oceanic crust can be seen to dip consistently landward, and the trench sediment is little disrupted in the approach of the decollement supporting the supposition that subduction is active in a nonaccretion mode along the Taitao and Tres Montes peninsula transect. The Pliocene Cabo Raper pluton (Figure 3) which is located west of the Taitao and Tres Montes peninsulas, has a culminating point (800 m above sea level) <2 km from the shoreline. The dip slope between the culminating point and the shoreline is along the extension of the continental slope between 1750 and 2250 m water depth (detail map not shown), along the same transect. This suggests that the Cabo Raper pluton extends seaward to within 6-7 km landward from the trench axis.

7. Postsubduction Segment (47-48°S)

Seven seismic lines (15 to 21, Figure 2) were shot along the Golfo de Penas accretionary prism (Figures 19 and 20) in an area extending from the Tres Montes peninsula (47°S) in the north to the Isla Campana at 48°S (Plate 1). The area includes the Humboldt abyssal plain, the Mornington channel, deep-sea fan sedimentary bodies along the Chile trench axis, the lower slope accretionary prism, the upper slope ridges, and the upper slope basin. When compiled with the EM12 bathymetry and the acoustic imagery (not shown), the seismic data permit a three-dimensional interpretation of the structures and their evolution through time (Figures 20, 21a, 21b and 22).

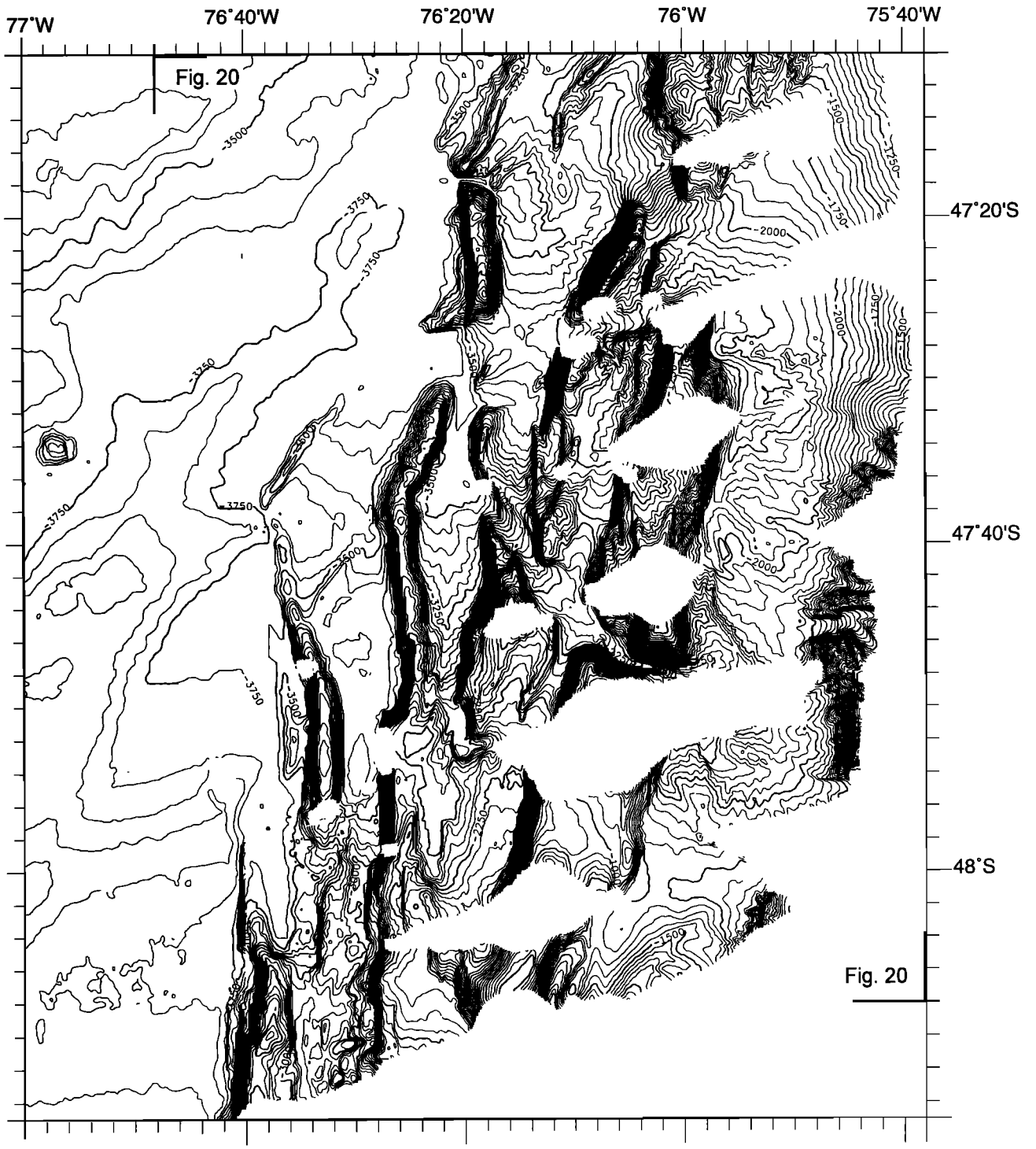

Figure 19. Bathymetric map (contours are every 50 m) of the Golfo de Penas accretionary prism along the postsubduction segment. Location of Figure 20 is shown. Location is shown on Plate 1.

The smooth flat seafloor imaged west of line 19 is part of the Humboldt abyssal plain which extends between the Pacific rise and the South American continental margin south of 47°S. Three volcanoes located at 77°W, 47°30'S (Figure 22) underline the crest of a N-S trending low ridge bounded by the depression paralleling the Tres Montes fracture zone (TMFZ, Figure 22) to the north. In line 18 (Figure 2), at about 77°W longitude (Figure 23), the sedimentary cover of the Antarctic plate exhibits a constant thickness of ~750-775 m. It can be divided into three units with different acoustic signatures labeled unit 1, 2, and 3 from bottom to top. Unit 1 can be divided into subunits 1A and 1B from bottom to top. They are 100-105 and 55-60 m thick, respectively. Subunit 1A consists of parallel strong reflections and constant thickness directly overlying the basement. Top of subunit 1B is underline by a strong reflection extending from lines 16 to 19 (not shown) over a distance of ~50 km. Subunit 1B exhibits an irregular thickness. It appears as channels scooping out the

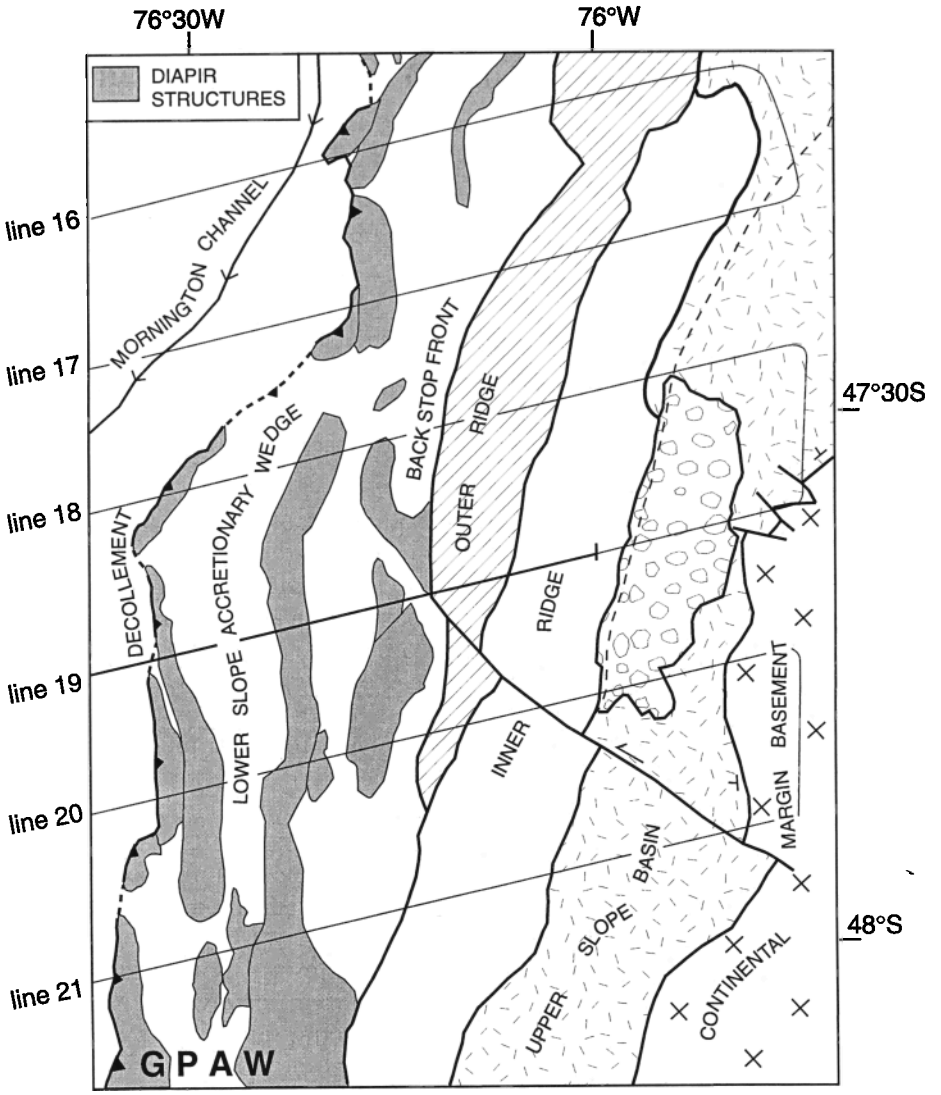

Figure 20. Sketch map showing the major morphostructural elements of the Golfo de Penas accretionary prism. Golfo de Penas accretionary wedge (GPAW). The area located east of lines 19 and 20 with irregular open dots shows a hummocky morphology interpreted as the signature of ice-rafted discharges. Location is shown on Figure 19.

subunit 1A. Unit 2 is composed of two subunits which are acoustically semitransparent. From bottom to top, subunits 2A and 2B are 70-75 and 100-105 m thick, respectively. Subunit 2A shows short-spaced coherent and thin reflections, while subunit 2B shows no coherent reflection. Unit 3 consists of a 425-430 m thick accumulation of mainly parallel and constant thickness reflections. In most cases, reflections are continuous over distances up to tens of kilometers. According to the magnetic age of the oceanic basement [*Leslie*, 1986; *Tebbens et al.*, 1997] we assume that units 1, 2, and 3 show a sediment record of the past 10 Myr.

The high backscatter which characterizes the Mornington channel in the acoustic EM12 imagery [*Bourgois et al.*, 1997] is interpreted as the signature of the rough sediment surface developed in association with the erosion and transport of detrital material along the channel. The Mornington channel is typically 5-10 km wide, exhibiting levees on either side. The main tributaries (Figure 22) are identified to be the South Taitao canyon and the Cabo Raper canyon to the north and the Golfo de Penas and the Cabo Bynoe canyons to the south. Since the South Taitao canyon and the Cabo Raper canyon show no connection to onland river systems, we assume that most of the detrital material bypassing the Mornington channel originates from the Golfo de Penas area today. Very strong reflections characterize not only the present-day sedimentation of the Mornington channel but also the sequence located beneath the channel. This 30-35 m thick sequence resulted from an accumulation of sediment infill of 1-2 to 10 m deep channels burrowed by sediment originating from the Mornington channel meandering along the Chile trench axis. Along line 19 (Figures 21a and 21b), the strong reflectors produced by the sediment accumulated along the Mornington channel can be followed landward not only beneath deep-sea fan IV but also farther to the east below the lower slope. The Mornington channel sequence appears as an heterochronous sequence that migrated seaward in relation to the development of both deep-sea fan IV and the lower slope accretionary wedge.

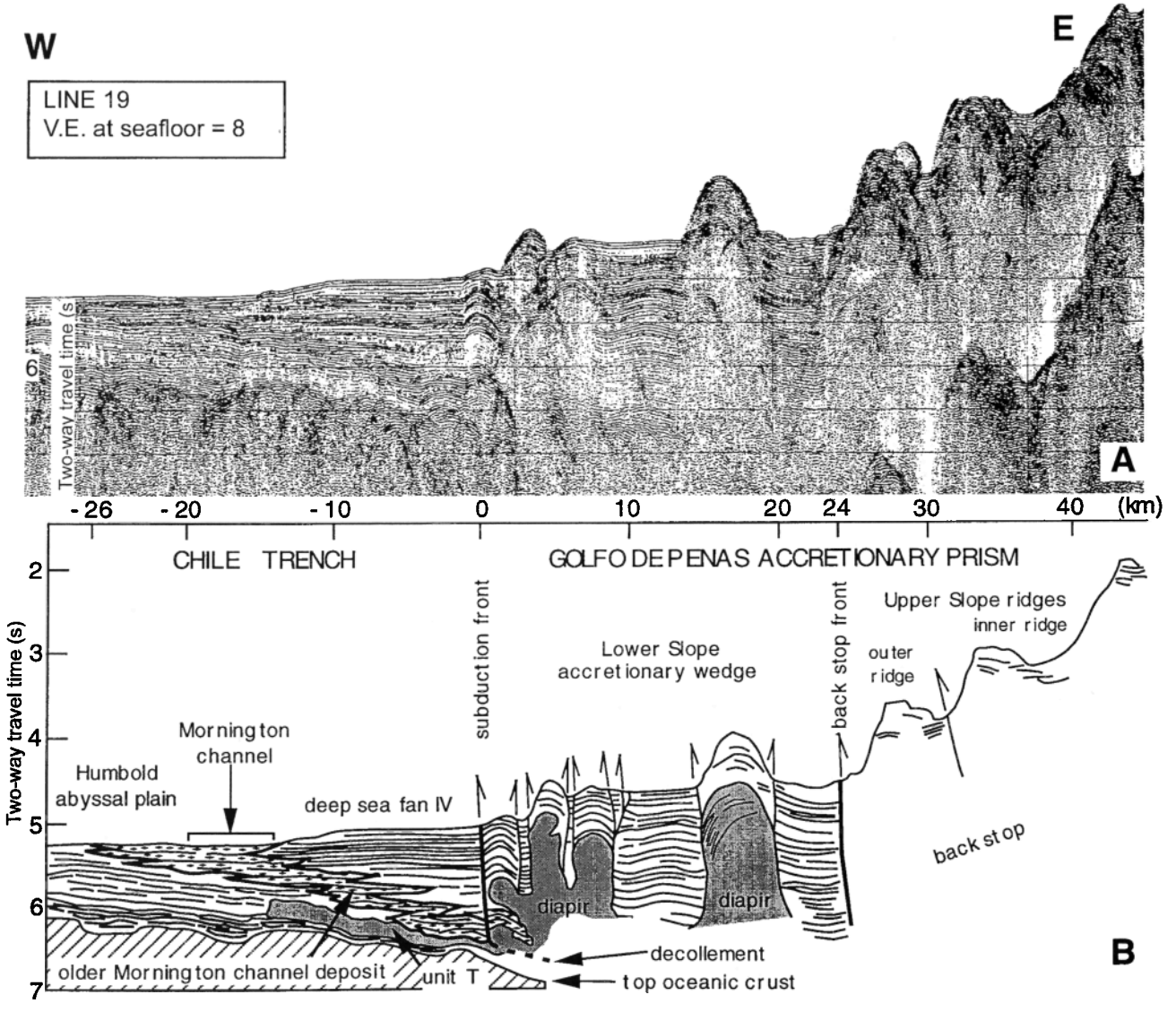

Figure 21. (a) Seismic line 19 along the Chile trench and Golfo de Penas accretionary prism. Horizontal scale marks the distance from the decollement in kilometers. (b) Line drawing showing the main sediment bodies and morphostructural elements of this area. Location is shown on Figure 22.

In the EM12 bathymetry (Figure 19) deep-sea fan IV (Figure 22) exhibits a typical lobe shape. It consists of a package of continuous reflections (Figures 21a and 21b) that range from subhorizontal to gently seaward dipping extending from the Mornington channel to the decollement at the toe of the lower slope. The seaward end of the fan wedge exhibits interfingering of fan turbidites with the Mornington channel sequences. To the east, the seismic facies of deep-sea fan IV can be followed through the lower slope to the backstop front, i.e., the front of the Upper Slope ridges domain (see below) acting as a buttress [*von Huene and Scholl*, 1991], over a distance of 50 km. To the east, the corresponding sequences are 1600 to 1900 m thick. The along-strike extension of deep-sea fan IV is ~40-50 km. Five imbricated deep-sea fans having a similar location both in space and time with respect to the main structural features of the area are identified. From north to south, they are termed deep-sea fans I, II, III, IV, and V (Figure 22). The typical high-amplitude reflectors of deep-sea fans III, IV, and V exhibit the original morphological signature with better preservation than those of deep-sea fans I and II reshaped by the Mornington channel cutoff. The crest of the fan-shaped body of deep-sea fans II, IV, and V that do show the distributary canyon outflow exhibits no connection to active canyons upstream. The decollement and the associated diapirs cut off the distributary channels of the deep-sea fans built into the abyssal plain. EM12 bathymetry allows us to follow the morphological crest of the deep-sea fan landward, along the Lower Slope accretionary wedge. Therefore we assume that building of the deep-sea fan building predates the tectonic development of the Lower Slope accretionary wedge. At the time the Lower Slope accretionary wedge began to form, Cabo Bynoe canyon, considered as the main tributary outflow for deep-sea fans III and IV, changed its course to flow along the present-day channel.

Below deep-sea fan IV (Figures 21a and 21b), the Antarctic plate sedimentary cover exhibits a mostly transparent seismic facies (unit T hereafter) with some parallel configurations of poor continuity and low amplitude in its lower part. Unit T

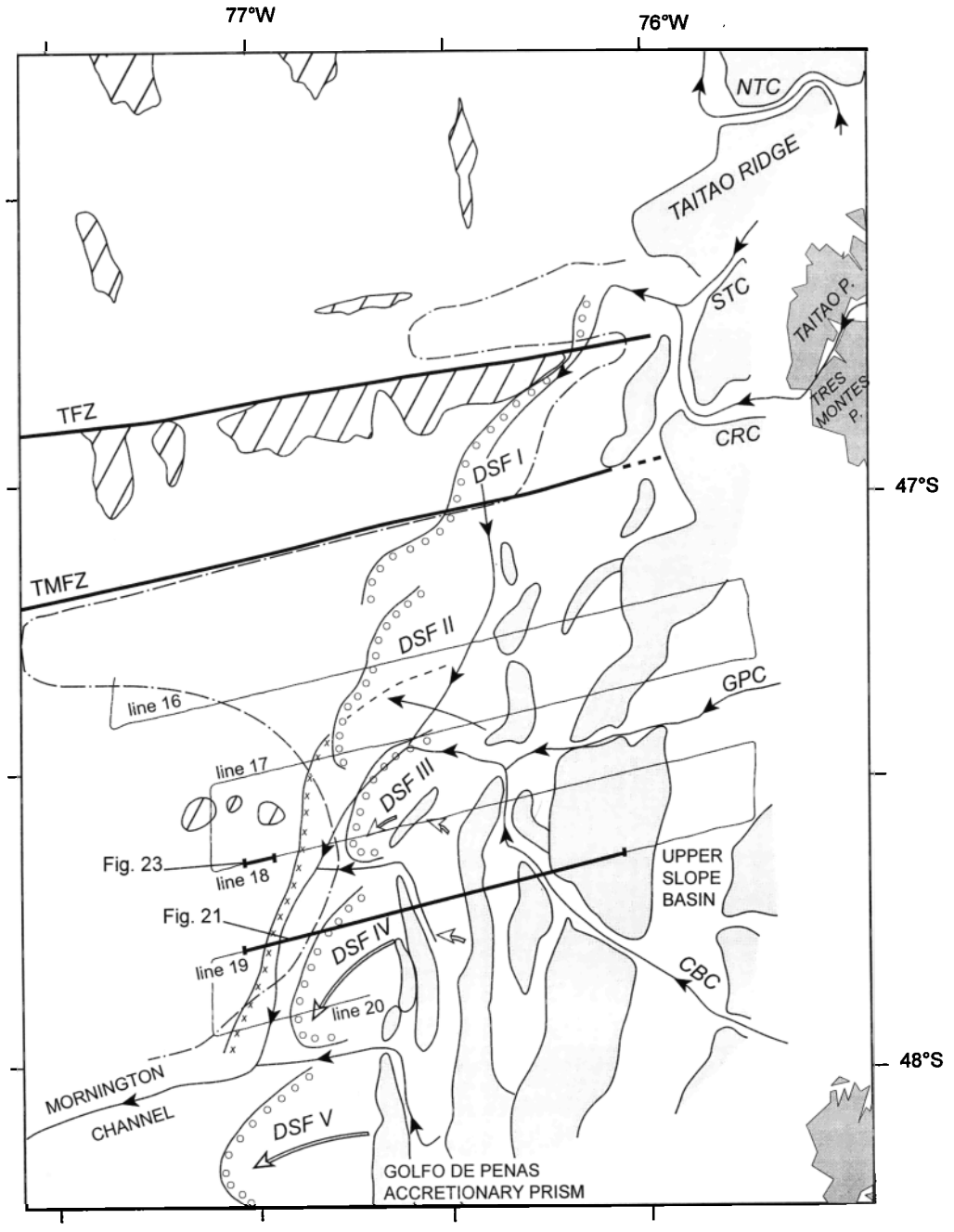

Figure 22. Main drainage (line with solid arrows) bypassing the Golfo de Penas accretionary prism today and deep-sea fans (open dots are seaward limit and open arrows are crest of fan body) along the Chile trench south of the Taitao Ridge. Cabo Bynoe canyon (CBC); Cabo Raper canyon (CRC); deep-sea fans I to V (DSF I to DSF V, open dots are seaward limit); Golfo de Penas canyon (GPC); North Taitao canyon (NTC); South Taitao canyon (STC); Taitao fracture zone (TFZ); Tres Montes fracture zone (TMFZ). Crosses along line show the seaward limit of the Mornington channel deposit; Dash-dotted line shows the seaward limit of the transparent layer unit T, dark pattern is the main morphostructural relief of the Golfo de Penas accretionary prism, diagonal shading shows the main Antarctica plate relieves. Locations of Figures 21 and 23 are shown. See text for more details. Location is shown on Plate 1.

extends widely (Figure 22) throughout the surveyed area: (1) from line 12 to 21 over a distance of ~150 km in a N-S direction and (2) from the backstop front to a seaward limit determined by the Antarctic plate morphology. North of the Taitao fracture zone, unit T overlies an oceanic crust younger than anomaly 2. Moreover, the boundary between Chrons 1n and 1r identified by *Leslie* [1986] and *Tebbens et al.* [1997] at 46°S extends southward to the Taitao fracture zone, in an area where unit T exists. We infer that unit T is Lower Pleistocene at the oldest and can be possibly as young as 1 Ma.

The Golfo de Penas accretionary prism (Figures 19, 21, 22, and 23) exhibits two different domains with distinctive

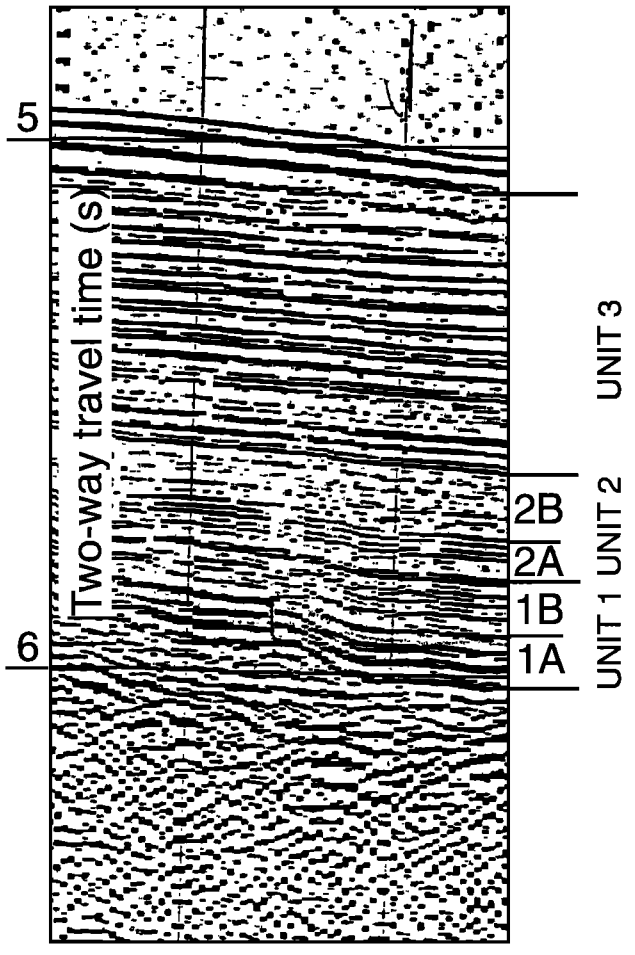

Figure 23. Seismostratigrafy of the Antarctica plate sedimentary cover from seismic line 18. See text for more details. Location is shown on Figure 22.

morphological signatures: (1) the Lower Slope accretionary wedge located seaward shows a structural pattern that consists of elongated ridges separated by relatively flat basins trending N-S with a 3° mean slope angle and (2) to the east the Upper Slope Ridges domain exhibits a N15-20°E trend and a 6° mean slope angle. The Upper Slope Ridges domain which extends over a distance of ~100 km consists of two massive ridges: the Outer and the Inner ridges. The crest of the Outer ridge is in water depth of about 2000 m below sea level, i.e., 1000-1250 m higher than the basins of the Lower Slope accretionary wedge; meanwhile, the Inner ridge crest is in ~750-1000 m water depth.

The elongated ridges of the Lower Slope accretionary wedge (line 19, Figures 21a and 21b) show roots in diapirs at depth. The transparent seismic facies with no clear reflector making the main body of the diapirs connects downward to unit T which probably consists of undercompacted mud. The frontal decollement also clearly connects to a diapir structure at depth, showing that unit T played a peculiar role in the tectonic style and evolution of the Lower Slope accretionary wedge. The flat basins located between the elongated ridges exhibit very weak deformation at depth and no significant differences in the amount of deformation with depth indicating that the deformation of this area post dates the most recent sediment covering the deep-sea fans, i.e., deep-sea fan IV along line 19. Moreover, the two main basins located along line 19 show no significant differences in their deformation, both suffering a similar amount of deformation and uplift. Tectonic deformation of the Lower Slope accretionary wedge is mainly concentrated along the diapir structures. They accommodated most of the convergence between Antarctic and South American plates that occurred after deep-sea fan accumulation. The uplift of the frontal diapir structure associated with the decollement (Figures 21a and 21b) can be estimated from the upward shift of the Mornington channel sequence at depth. The amount of displacement along the decollement is ~40-50 m at this site. When associated with the state of deformation of the frontal diapir, it suggests that deformation began recently at this site. Conversely, the more evolved deformation of diapirs located landward, as shown by no clear reflection occurring at shallow depth, suggests that deformation began earlier landward. Although the frontal diapir shows a more evolved signature along strike (for example, along line 20, not shown), we assume that deformation began earlier landward as also suggested by a higher uplift of inner diapir structure. However, the EM12 imagery shows active erosion occurring along all elongated ridges, suggesting that all diapir structures are suffering active uplift. Therefore active shortening exists not only along the decollement but also throughout the Lower Slope accretionary wedge, along the diapirs structures. The mean total net shortening of the Lower Slope accretionary wedge calculated along lines 17 to 21 is ~3 km. If we consider that the lower slope shortening accommodates the whole 2.4 cm/yr net convergence between the Antarctica and the South America plates, its deformation would begin at 125 ka at the earliest.

The Outer ridge and the Inner ridge of the Upper Slope ridges domain form a prominent relief which is a major barrier for detrital material originating from the Golfo de Penas area. The Golfo de Penas and the Cabo Bynoe canyons (Figure 22)

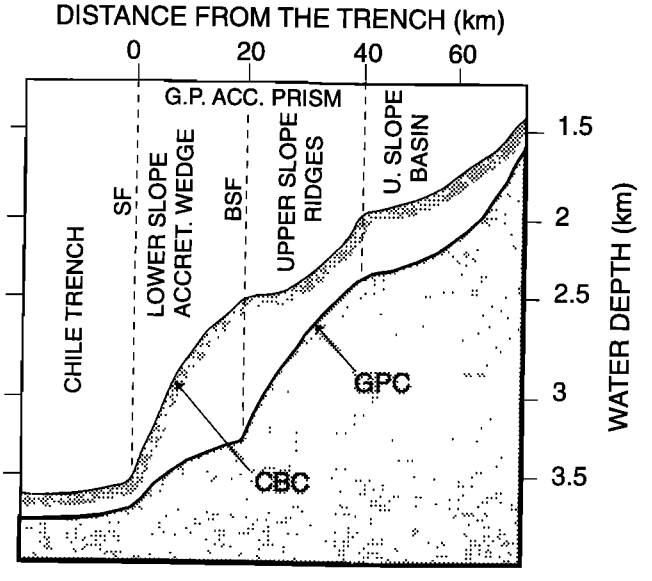

Figure 24. Long profile of the Golfo de Penas canyon (GPC) and Cabo Bynoe canyon (CBC) along their courses across the Golfo de Penas accretionary prism. Back stop front (BSF), subduction front (SF). See text for more details. Locations of canyons are shown on Figure 22.

cutting across the Upper Slope ridges belong to one of the major transverse routes to sediment feeding into the Chile trench. They connect to the east to the onland river system of the Rio Baker (Figure 4) which drains the Argentina Andean foothills. Therefore the Rio Baker river system and its offshore distributary prolongation are antecedent drainage with respect to the uplift of both the Andes and the Upper Slope ridges. The long profiles (Figure 24) of the Golfo de Penas and Cabo Bynoe canyon (Figure 22) show three main downstream slope breaks bounding four different sections that characterize the morphotectonic domains of the Golfo de Penas accretionary prism, from east to west: (1) a section with a rather steadily decrease of the slope downstream typical of the Upper Slope basin, (2) a section with a steeper mean channel slope and major differences in the general shape of the long profile of the two canyons that characterized the Upper Slope ridges domain, (3) a steep section with an upward convex long profile across the lower slope, and (4) a flat section along the Chile trench axis. The long profile of the Upper Slope basin is consistent with relative subsidence of this area as regard the adjacent downstream domain. The sediments are actively trapped in the Upper Slope basin. Along the Golfo de Penas canyon, the steep gradient of the slope and the upward convex shape of the long profile of the Upper Slope ridges domain are indicative of active deformation and uplift. Along this transect, the major fault of the Golfo de Penas accretionary prism, evidenced from the main slope break, is located at the back stop front. Along the Cabo Bynoe canyon, the main slope break occurs west of the Lower slope accretionary wedge at the subduction front. Here the tectonic deformation is actively transferred westward, from the back stop front to the subduction front. The major fault at the Inner ridge-Outer ridge boundary is not associated with a break in the slope gradient along the stream of both canyons. We assume that this fault has no significant tectonic activity today. The Outer and Inner ridges are acting as a distinct block with regard to the active uplift of the Upper Slope ridges domain. Since the Outer and the Inner ridges are along the southward prolongation of the Taitao and Tres Montes peninsulas, respectively, we speculate that basement rock cropping out on land may extend offshore along the upper slope ridges. It should also be noted that the Taitao and Tres Montes peninsulas are both actively uplifting [*Bourgois et al.*, 1996].

8. Discussion

The previous investigations of the Chile triple junction area indicated that the landward trench slope is severely eroded by the approach of the Chile ridge crest and that the continental margin is rebuilt following ridge subduction [*Cande and Leslie*, 1986; *Cande et al.*, 1987; *Behrmann et al.*, 1992a; *Behrmann et al.*, 1994]. This is apparent from (1) the southward narrowing and steepening of the continental margin as the triple junction is approached from the north and the broadening of the margin along the Golfo de Penas accretionary prism south of the triple junction, and (2) the reconstruction of an accretionary prism along the North Taitao canyon subsegment immediately south of the triple junction. The data collected during the CTJ cruise document a much more complex evolution. During the past 1 Myr, the tectonic regime along the Andean convergent margin in the area of the Chile triple junction experienced major instabilities both through space and time. Two main non-steady state processes have operated along this segment of the margin: (1) the episodic input of sediment to the trench axis in relation with the evolution of the Andean ice cap, and (2) the tectonic reorganization at the Nazca-Antarctica plate boundary associated with the Chile ridge subduction. These two processes and their interaction largely determine the tectonic regime of the continental margin (subduction-erosion versus subduction-accretion) and its evolution through time. However, the topography of the subducting Antarctica plate is suspected to have importance in both creating the major reentrant south of the Taitao ridge and the active uplift of the Taitao and Tres Montes peninsulas. Also, the thick accretionary prism imaged along the Taitao ridge transect allows us to better identify the processes that induced ophiolite emplacement, i.e., obduction, into the continental margin. Another major thematic question of the Chile margin triple junction area is that of the Bahia Barrientos ophiolite emplacement as highlighted from the Taitao ridge structure.

8.1. Sediment Supply

The seismic lines along the postsubduction segment document an episodic development of the Golfo de Penas accretionary prism. The accumulation of more than 50% of deep-sea fans I to V along the Lower Slope accretionary wedge began at 125 ka at the earliest. The tectonic style which is similar to other rapidly accreting margins with thick trench accumulation, for example, along the Aleutian arc [*McCarthy and Scholl*, 1985], is deeply marked here with diapirism. Diapirs root at depth in a layer with a transparent seismic signature, i.e., the unit T, probably composed of undercompacted mud. Along line 19 (Figure 21), frontal accretion added almost all the trench fill section to the lower slope. Offset of trench turbidites clearly defines the frontal thrust. This thrust deeply penetrates the trench sequence down to unit T where it is supposed to sole into the decollement. We assume that much of the incoming trench material was accreted in front of the Upper Slope ridge back stop. Only the Antarctic plate sediment cover below unit T was eventually underthrust beneath the backstop. Along line 19, frontal accretion added 0.8 to 1.8 km of the trench fill sediment to the toe of the continental margin. Reconstructing the situation before tectonic deformation of the Lower Slope accretionary wedge (Figure 25) allows us to show that the horizontally stratified turbidites extended from the Mornington channel to the back stop front at the toe of the Upper Slope ridges. In map (Figure 26), this reconstruction shows that deep-sea fan IV connected upslope directly to the outlets of the Golfo de Penas and Cabo Bynoe canyons. Moreover, since the convergence between the Antarctic and South America plates left no significant tectonic record in the trench section beneath unit T, we infer a very rapid trench sediment accumulation. We suggest (see section 4) that deep-sea fans (i.e., at least deep-sea fans II, III, and IV) formed during the interglaciation isotopic substage 5e, circa 130 to 117 ka, when the Rio Baker river system was free of ice allowing sediment supply to the trench. The continental margin at 130-117 ka (Figures 25 and 26) which extended seaward to the backstop front, i.e., the toe of the Upper Slope ridges, was only 30 to 35 km in width, about half the present width. Before deep-sea fans II-IV accumulated (Figure 25c), during the glacial $\delta^{18}O$ isotope stage 6 (circa 150 to 200 ka) when the Patagonian ice sheet prevented massive trench fill, the trench

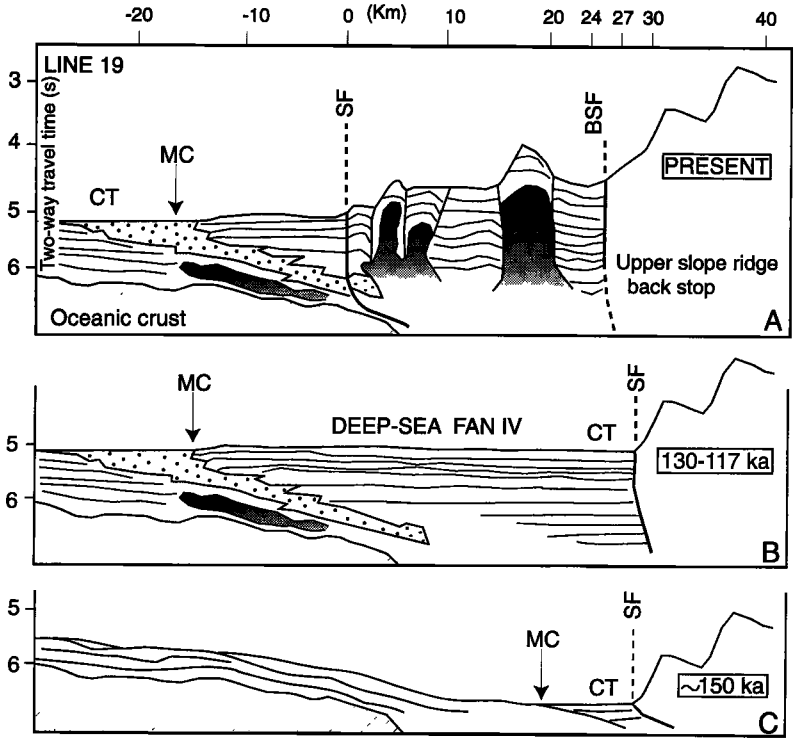

Figure 25. Tectonic and detrital input history of the Chile trench (CT) along the postsubduction segment (reconstruction along line 19, see Figure 22 for location). Back stop front (BSF); Subduction front (SF); Mornington channel (MC). Note that (1) the subduction front at 150 ka (Figure 25c) and 130-117 ka (Figure 25b) coincides with the back stop front today (Figure 25a) and (2) the subduction front migrated 24 km to the west during the past 130-117 kyr. See text for more detail.

floor was deeper than today, maybe as much as 1-1.5 km. During $\delta^{18}O$ isotope stage 6 the South America convergent margin south of the Chile triple junction was narrower and much deeper at its seaward edge than today. It exhibited nonaccretionary or erosional mode characteristics. The massive input of detrital sediment to the trench axis during interglaciation isotopic substage 5e appears to be the major factor determining the tectonic regime change from subduction-erosion to subduction-accretion. Along this specific section of the Chile trench the tectonic regime of the Andean continental margin is strongly determined by climatic factors. During the past 150 kyr, the stress regime change along the postsubduction segment was coeval with a major uplift of the Upper Slope ridges domain with a rate of about 1 cm/yr, required to sustain the 6° value for the mean slope angle of this domain today.

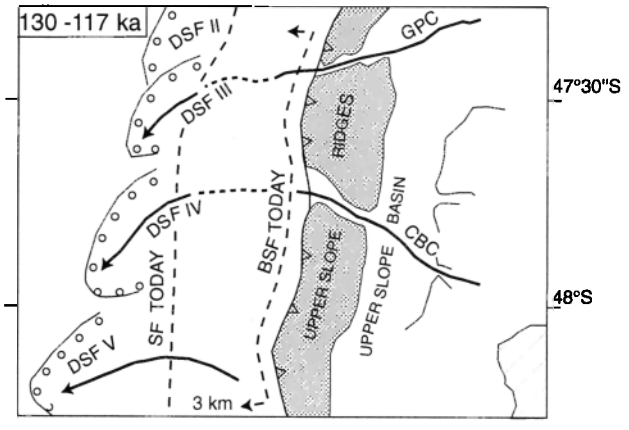

Figure 26. Reconstruction of the Chile continental margin and trench along the postsubduction segment at 130-117 ka. At that time, the decollement was located along the toe of the Upper Slope ridges. The deep-sea fans (DSF) III and IV connected with the outflow of the Golfo de Penas and Cabo Bynoe canyons, respectively. The dashed lines show the present location of the subduction front (SF) and the back stop front (BSF) resulting from 3 km of convergence between the Antarctic and South America plate during the past 130-117 kyr. Cabo Bynoe canyon (CBC); Golfo de Penas canyon (GPC). See text for more detail.

Along the presubduction segment, there is a conspicuous discrepancy between the compressive Chile trench and the adjacent extensional continental margin tectonic regimes. One of the critical factors that could help to explain the apparent paradox is a major increase in trench sedimentation. Recent and current accretion in the trench would reflect a recent and rapid influx of trench sediment, while the extensional tectonic regime of the continental margin which is generally supposed to be associated with subduction-erosion at depth would be a remnant of the previous situation with a low supply of sediment to the trench axis. Today the tectonic regime of the Chile continental margin north of the triple junction is at the turning point from subduction-erosion to subduction-accretion with both regimes active at the same time. Massive accretion of trench sediment will occur in the near future, reproducing the situation described to the north [*Bangs and Cande*, 1997] at 38°S. In this area located 800 km north of the Chile triple junction we assume that the influx of sediment began earlier in relation with an older retreat of the ice cap that

resulted in a 2-3 times thicker trench sediment accumulation. As proposed by *Bangs and Cande* [1997], we suspect that accretion occurring today along the presubduction segment is linked to a dramatic increase in trench sediment supply. We suggest that the change in tectonic regime of the continental margin along the presubduction segment is climate-induced as it is along the postsubduction segment.

8.2. Tectonic Reorganization at the Nazca-Antartica Boundary

During the CTJ cruise, no additional complexity was found in the magnetic lines collected along the CRS 1 transect, as compared to magnetic data reported in previous works [*Herron et al.*, 1981; *Tebbens et al.*, 1997]. The western flank of the CRS 1 recorded an apparently continuous anomaly sequence from the central anomaly to anomaly 2A. There is no evidence in the magnetic data to question the subduction history of the CRS 1 as currently accepted: the Chile triple junction defined by the CRS 1 and the trench migrated northward from 46°25'-46°30'S to its present location at 46°09'S during the past 200-300 kyr. However, this simple reconstruction leaves three major points at issue: (1) Along the Chile ridge subsegment, the lack of sediment accumulation strikingly characterizes the CRS 1 axial valley in contrast to the Chile trench in its southward prolongation and the adjacent oceanic crust west of them. The reduced supply of detrital material that transits today through the North Taitao canyon does not properly explain this situation. Since the rift fault system of the CRS 1 sharply cuts off the thick accumulation of trench sediment south of the Chile triple junction and the thick accumulation of sediment overlying the oceanic crust that lies directly west of the rift valley wall, we suspect that an age gap exists between the axial valley floor and the adjacent oceanic crust. (2) The Antarctica plate area located both to the west and to the south-west of the CRS 1 axial valley exhibits a fault network which evolved through two extensional tectonic pulses, not documented elsewhere in the surveyed area. Moreover, in the vicinity of the triple junction (Figure 8), the rift fault system of the CRS 1 trending N10°W sharply cuts off the nearly north-south trending fault network which characterizes the Chile trench in this area. (3) The complex structure of an accretionary wedge documented along the Taitao ridge transect shows no extension to the north. The tectonic history of the Chile continental margin is different on either side of the North Taitao Ridge fault bounding the Taitao Ridge to the north.

A better understanding of these three major points can be achieved by considering the CRS 1 as evolving through a recent westward jump to its Present location (Figure 27). This ridge jump accounts for the age gap which is suspected between the CRS 1 axial valley and the Antarctica adjacent seafloor and the two extensional tectonic pulses documented in this specific area. We assume that the older extensional faults developed during a first phase of ridge subduction in relation to the development of the associated slab bulge. Then the westward ridge jump occurred, resulting in the CRS 1 development in its present location. Subsequently, the rift-related tectonic activity of the CRS 1 induced the development of a new fault network and the bulge-related older fault reactivation. Moreover, this model allow us to propose a coherent reconstruction of the margin area located between the Darwin and Taitao fracture zones, including the Taitao Ridge

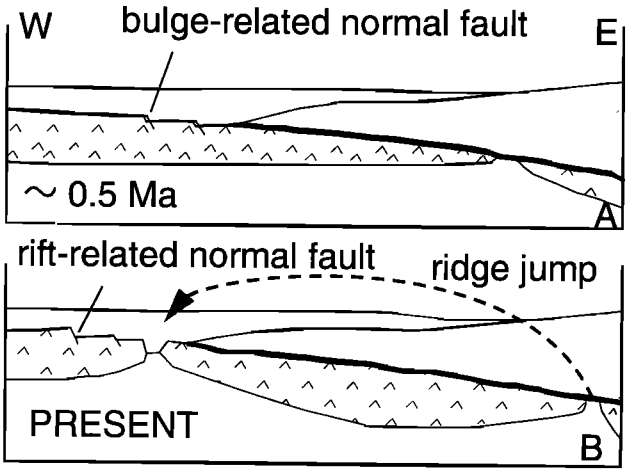

Figure 27. (a) Chile ridge subduction occurred sometime after 780 ka. As the Antarctica plate entered the subduction, bulge-related normal faults developed. (b) Ridge jump to the west occurred subsequently, resulting in the development of the CRS 1 in an area of the Antarctic plate previously deformed by bulge-related normal faults. Then tectonic deformation associated with spreading activity along the CRS 1 occurred. A rift-related normal fault network developed resulting in the reactivation of the older bulge-related fault network. Diagonal pattern indicates Andean continental margin; arrowhead pattern indicates oceanic crust; spreading center (SC); not to scale. See text for more detail.

accretionary wedge. Since no signature in the magnetic records exists, the ridge jump had to occur during the last Brunhes normal polarity event, i.e., Chron C1n, that is to say after 780 ka [*Cande and Kent*, 1992]. Because the ridge-parallel tectonic fabric of the Antarctic plate was reactivated not only west of the CRS 1 but also west of the trench axis in its southward prolongation, we assume that ridge jump took place between the Darwin fracture zone and the North Taitao Ridge fault.

The North Taitao Ridge fault which offsets the subduction front right laterally by ~25 km shows no clear evidence of such a large strike-slip movement along its seaward and landward prolongations and has the characteristics of a transform fault. Moreover, it also exhibits a significant normal slip component with a downward offset of the Taitao Ridge. This is in good agreement with the Antarctic plate subsidence south of the flexure along the seaward prolongation of the North Taitao Ridge fault. Since no major contractional feature exists along the North Taitao Ridge fault, we assume that convergence along the frontal decollement trends parallel to the fault on either side of it. Therefore, there is a discrepancy between the regional and the local convergences between the Antarctic and South America plates that trend N90°E [*DeMets et al.*, 1990] and N50°E, respectively. The E-W trending thrust fault system which offsets the subduction front in an area north of point X (Figure 13b) is believed to compensate for the northward component associated with the local N50°E trending convergence. North of the North Taitao Ridge fault, in the Taitao canyon area, the width of the accretionary prism decreases abruptly to only 5-6 km, and the apex of the back stop is 1000 m deeper as compared to the Taitao Ridge transect (AB, Figure 16). We infer that the tectonic history of the Chile continental margin is different on either side of the North

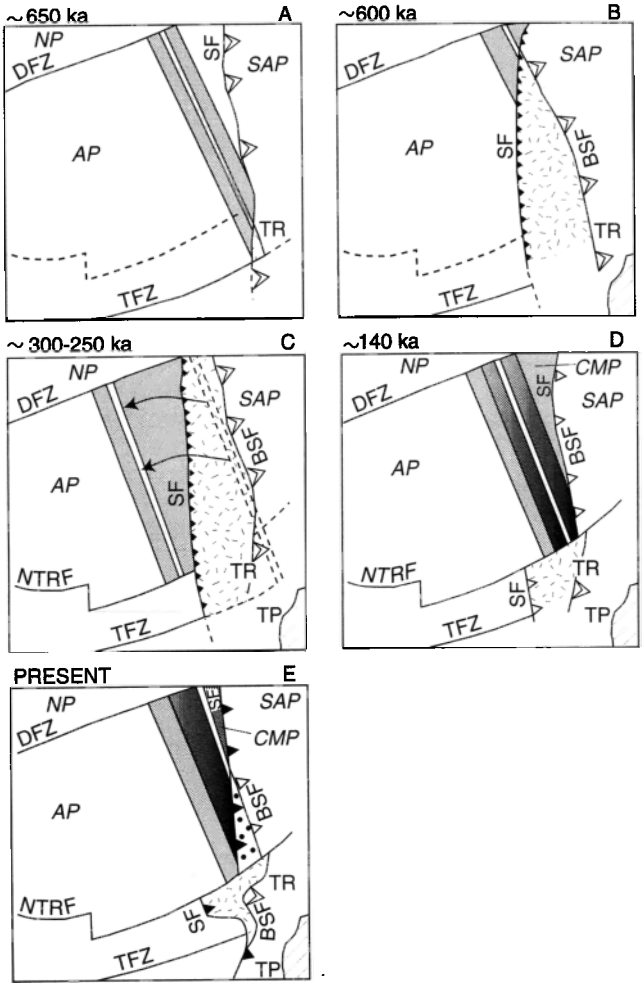

Figure 28. Reconstruction of ridge subduction history along the transect located between the Taitao and Darwin fracture zones and tectonic model of birth and death of the ephemeral Chonos microplate. During the past 780 kyr, two ridge-subduction phases separated by a westward ridge-jump occurred. This evolution controlled the tectonic regime of the adjacent continental margin with two steps of subduction-accretion separated by subduction-erosion. South of the North Taitao Ridge fault, no ridge jump occurred, allowing the previously constructed accretionary prism to be preserved along the Taitao Ridge. See text for more detail. Antarctic plate (AP); Chonos microplate (CMP); Darwin fracture zone (DFZ); Nazca plate (NP); North Taitao Ridge fault (NTRF); South America plate (SAP); Taitao fracture zone (TFZ); Taitao peninsula (TP); Taitao ridge (TR); triangles, subduction front (SF) and back stop front (BSF); double lines, active spreading ridges; solid arrows, westward ridge jump; dashed pattern and solid dots, first and second accretionary prism, respectively; light shaded areas, oceanic crust accreted between 780 and ~300 ka; dark shaded areas, accreted oceanic crust younger than ~300 ka.

Taitao Ridge fault with a well-developed accretionary prism along the Taitao Ridge transect but showing no prolongation north of it. The along-strike downward shift of the decollement of 1000 m south of the North Taitao Ridge fault suggests that the Taitao Ridge accretionary prism extended northward and was subsequently removed north of it. We suggest a tectonic evolution as shown on Figure 28. Sometime after 780 ka (Figure 28a), a first subduction of the Chile ridge segment occurred between the Taitao and the Darwin fracture zones. As the Chile triple junction migrated to the north, an accretionary prism (Figure 28b) was rebuilt south of it. We assume that the thrust sheets accumulated along the Taitao Ridge transect are a remain of this old accretionary prism. When in the ridge-trench-trench configuration, the triple junction migrates at a rate of 160 cm/yr. Therefore it took <50 kyr for the ridge segment to subduct totally. At about 300-250 ka, a section of the Chile ridge located between the North Taitao Ridge fault and the Darwin fracture zone jumped west of the subduction front (Figure 28c) along the Present CRS 1, in an area of the Antarctic plate younger than 780 ka. This ridge jump created an ephemeral microplate (the Chonos microplate), as proposed elsewhere by *DeLong and Fox* [1977]. The Chonos microplate boundaries are the CRS 1, the Darwin fracture zone, the Chile trench, and the North Taitao Ridge fault. The subduction of the Chonos microplate was associated with frontal subduction-erosion that removed most of the previously accumulated accretionary prism. South of the North Taitao Ridge fault, no ridge jump occurred (Figure 28d) preventing subduction erosion along the Taitao ridge transect (Figure 28e). As the Chile ridge (i.e., the CRS 1 which is the western boundary of the Chonos microplate) reached the trench again, the triple junction changed from a transform-trench-trench to a ridge-trench-trench configuration. The section of the margin south of the triple junction began to develop an accretionary prism; meanwhile, the northern section stayed in a subduction-erosion mode, as it is today.

8.3. Topography of the Ocean Floor

Since the trench axis is devoid of sediments along the Chile ridge subsegment, we infer not only that the source of detrital material accumulated along the presubduction segment was located to the north but also that the slab segmentation determined the locus of trench sediment accumulation. The Chile ridge relief entering the subduction appears to be damming the sediment originating from the north. South of the Darwin fracture zone, no subduction-accretion occurs because no sediment is entering the subduction today. Conversely, north of the Darwin fracture zone, the along-strike deepening of the trench axis basement allowed the detrital sediment originating from the north to accumulate and therefore subduction-accretion to be active. The Chile ridge considered as a relief diverting the sediment supply to the trench plays a major role in the tectonic development of the continental margin. From ODP Leg 141 data, *Behrmann et al.* [1994] have shown that no frontal accretion of sediment has occurred along the Chile ridge subsegment since the late Pliocene. At ODP Site 863 (Figure 8b), most of the material accreted during the Pliocene was subsequently removed by subduction-erosion. As along the northern Taitao canyon, the continental basement extends to within few kilometers landward from the trench axis, indicating that considerable volume of forearc basement has been tectonically eroded in an area where the Chile ridge is supposed to be at depth. This factor adds the role of the Chile ridge as a thermal-induced relief, which diverts sediment. Subsidence of the margin should also be expected from subduction-erosion related to ridge subduction at depth.

At the toe of the Taitao Ridge accretionary prism, active subduction of trench sediment is occurring in relation to trench infill compressional deformation. Today, the thick trench infill is actively underthrust landward below a subhorizontal frontal decollement. The frontal decollement slices the three thrust sheets of the Taitao Ridge accretionary prism horizontally at their base indicating that (1) frontal subduction-erosion also occurs today and (2) the Taitao ridge accretionary prism grew during an older phase during a different tectonic regime at the subduction front. Since the frontal decollement follows the same 3250 m water depth isobath on both side of the South Taitao canyon, we infer that active subduction occurs farther to the south beneath a flat lying decollement, along the Taitao and Tres Montes peninsula transect. Along the reentrant at 46°40'S, the trench fill shows little tectonic deformation; meanwhile, thrust faulting of the trench fill exists to the north and to the south. A slight change in the dip angle of the oceanic basement from subhorizontal to a clear landward dipping may explain the weakness of active tectonic deformation along the reentrant off the Taitao and Tres Montes peninsulas. The scar associated with this major reentrant is in the landward prolongation of the Taitao Fracture Zone ridge (Plate 1). Thus it exhibits the characteristics of an impacting seamount that accelerates removal of material from the front of the margin. We speculate that a ridge crest located between the Taitao and Tres Montes fracture zones in the landward prolongation of the Taitao Fracture Zone ridge underthrust beneath the Chile continental margin. The underthrusting action of such a large edifice not only wedges up, deforms, and fractures the base of the trench slope [*Lallemand and Le Pichon*, 1987] but also induces uplift of the overlying continental wedge. We suggest that the major uplift of the Taitao and Tres Montes peninsulas originates from a subducting seamount rather than being thermally induced by the presence of a Chile ridge segment beneath them or induced by the reconstruction of an accretionary prism [*Bourgois et al.*, 1996]. This is in good agreement with the absence of significant frontal accretion acting at the toe of this subsegment of the margin today. This hypothesis fits also with the uplift and subsidence history as recorded by the Pliocene and Pleistocene sediments of the Taitao and Tres Montes peninsulas [*Bourgois et al.*, 1996].

8.4. Ophiolite Emplacement

A major thematic question of the Chile margin triple junction area is that arising from the Taitao Ridge (Figure 1) which is supposed to be the seaward prolongation [*Bangs et al.*, 1992] of the onland Bahia Barrientos ophiolite (Figure 3) cropping out in the Taitao peninsula. The previous results published by *Kaeding et al.* [1990] and *Le Moigne et al.* [1996] that document an oceanic origin for peridotites and gabbros of the Bahia Barrientos ophiolite substantiate this assumption. From drilling material recovered during Leg 141 at Site 862, *Behrmann et al.* [1994] subsequently suggested that the Taitao Ridge is a nascent forearc ophiolite emplacement of which is connected with the Taitao fracture zone. It may constitute an ophiolite terrane in the process of emplacement.

The EM12 data and seismic lines collected along the Taitao Ridge during the CTJ campaign have revealed the complex three-dimensional structure of an accretionary wedge (Figure 13b) including at least three sheets: two thrust sheets at the seaward edge of the ridge and a thick midslope thrust sheet landward. This accretionary wedge stacked beneath the Chile continental margin back stop is 25-28 km in width. Along the Taitao Ridge, the back stop apex (BSA, Figure 13a) is located 16-17 km seaward from the Taitao peninsula shoreline, to 75°54'W in water depth as shallow as 1500 m. As the prism grew, the wedge beneath the back stop was underplated causing uplift of the apex. The midslope thrust sheet exhibits a volcanic basement with petrological, geochemical, and mineralogical signatures consistent with an oceanic origin [*Guivel et al.*, 1999] and a well-stratified sedimentary cover with a seismic signature similar to that of the adjacent Antarctic plate. We propose that the tectonic accretion of a slice of ocean floor occurred along the Taitao Ridge transect during the past 780 kyr. However, the midslope thrust sheet is stacked up beneath a back stop consisting of volcanic rocks and sediments [*Behrmann et al.*, 1994; *Forsythe et al.*, 1995] similar both in composition and age to those cropping out onshore in the Taitao peninsula. Therefore a major thrust fault must separate the midslope thrust sheet from the Taitao peninsula rock units including the Bahia Barrientos ophiolite. Indeed, a major age gap exists between the two pieces of ophiolite. The Bahia Barrientos ophiolite is older than 6-4 Ma (i.e., older than the 6-4 Ma intruding Cabo Raper pluton [*Mpodozis et al.*, 1985; *Guivel et al.*, 1999]); meanwhile, the midslope thrust sheet ophiolite along the Taitao ridge must be younger than 780 ka. We assume that these two pieces of ophiolite have no connection in both space and time. While the process of emplacement of the midslope thrust sheet ophiolite along the Taitao ridge is understood, that of the Bahia Barrientos remains unsolved. However, it is probably reasonable to think that processes at the origin of the emplacement of both pieces are similar.

9. Conclusion

Along the specific section of the Andean continental margin surveyed during the CTJ cruise, two main factors controlling the tectonic regime have been identified. The trench accumulation is strongly controlled by climate variation and the tectonic reorganization at the Nazca-Antarctica plate boundary which involved postsubduction ridge jump associated with the evolution of the Chile triple junction. Underthrusting of slab positive topography also locally influenced the tectonic evolution of the continental margin. The combination of these three unconnected factors and their fluctuation through time determine the dominant tectonic regime of a peculiar segment of the continental margin at any particular time.

Rapid increase in trench deposition caused the margin to switch from subduction-erosion to subduction-accretion (1) after the glacial-interglacial episode at 130-117 ka along the postsubduction segment and (2) after the last deglaciation along the presubduction segment. Both situations are related to major retreat of the Andean ice cap, allowing continental river drainage to feed the trench axis with sediment. Conversely, a nonaccretion or a subduction-erosion mode characterized the presubduction and postsubduction segments during glacial maximums. The tectonic regime of the Andean continental margin is climate-dependent. In the area of the Chile triple junction the duration of climatic cycles and their magnitude and chronology greatly determine the episodes and

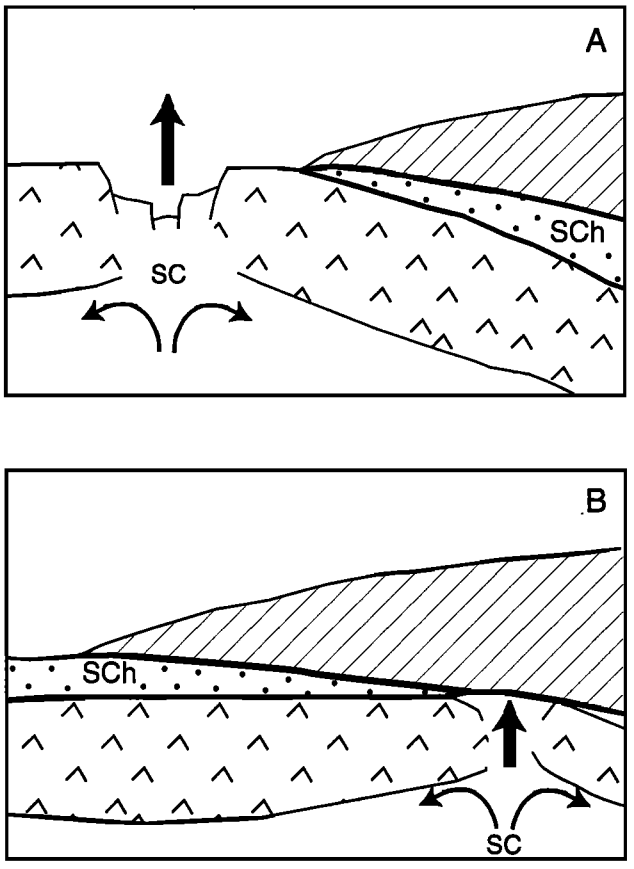

Figure 29. (a) Before ridge subduction the subduction channel (Sch, dotted pattern) is thickening arcward; no accretion of sediment is allowed. (b) After ridge subduction the subduction channel (Sch, dotted pattern) thins arcward; subduction-accretion works. See text for more detail. Diagonal pattern, Andean continental margin; arrowhead pattern, oceanic crust; spreading center (SC); thick solid arrow, active uplift.

timing of the Andean convergent margin development during the past 1 Myr.

The subduction history of the Chile ridge and transforms is not as simple as previously proposed [*Mpodozis et al.*, 1985; *Leslie*, 1986] for the past 1 Myr. North of the Taitao fracture zone, the current subduction of the CRS 1 follows a first phase of ridge subduction which occurred after 780 ka. The past 1 Myr tectonic evolution of the Chile triple junction reveals the same typical short-term instabilities and complexities which have been identified at other triple junctions such as Mexico [*Luhr et al.*, 1985; *Bourgois and Michaud*, 1991; *Hey*, 1998] or Queen Charlotte [*Rohr and Furlong*, 1995]. North of the Taitao fracture zone, the ridge subduction history has deeply influenced the tectonic evolution of the continental margin. Along the North Taitao canyon subsegment, two episodes of accretion separated by an episode of subduction-erosion occurred in <780 kyr. Moreover, the northward migration of the triple junction which occurred twice along this subsegment introduced an along-strike variation in the magnitude of accreted material and the duration of each tectonic episode along a specific transect.

A question to be addressed is the origin of the tectonic regime change of the continental margin from subduction-erosion to subduction-accretion in association with the Chile triple junction migration. In the presubduction situation (Figure 29a), the thin, buoyant lithosphere of the leading edge of the Chonos microplate is west of the subduction front. Therefore the subduction channel [*Cloos and Shreve*, 1996; *Charlton*, 1988] along the decollement is thickening arcward allowing the subducted material to be easily removed landward. As ridge subduction occurs, the buoyant lithosphere of the spreading center moves arcward beneath the overriding block. The descending plate acts to move upward and the shear zone to thin landward. Conversely, as regarding the presubduction situation, subducted sediment becomes accreted (Figure 29b) because of an increase in the pressure gradient acting to resist sediment subduction. We think that the subduction channel concept developed by *Shreve and Cloos* [1986] and *Cloos* [1992] for subduction of sediment and seamount asperities closely matches the evolution of the tectonic regime at the Chile triple junction area.

The westward ridge jump which occurred along the CRS 1 produced the ephemeral Chonos microplate north of the North Taitao Ridge fault. Slab weakness and thinning may have been introduced by this process of plate fragmentation. Breakup of the young, buoyant slab in the nearby subduction zone may have two potential consequences regarding (1) the emplacement of ophiolite slices into the accretionary prism, i.e., the continental margin, and (2) the contamination of basalts sampled along the Chile ridge [*Klein and Karsten*, 1995]. From anomalous trace element ratios they proposed that the back arc affinities of Chile ridge lavas erupted along the CRS 1 may have been produced by mixing of MORB melt with melts of mantle containing 0.35% sediment and ~3% altered oceanic crust contaminants. We suggest that slab fragmentation induced by ridge subduction increases oceanic crust alteration through multiple episodes of faulting and allows the suboceanic mantle to become contaminated with material derived from adjacent subduction.

Acknowledgments. We gratefully acknowledge the thoughtful and thorough reviews of two anonymous reviewers. The CTJ cruise was supported by IFREMER (France). We thank the captain and the crew of the R/V *L'Atalante* for their efficient work and the Servicio Hidrografico y Oceanografico (SHOA) de la Armada de Chile. This work was funded under grant 97N51/0353 by the Institut National des Sciences de l'Univers (INSU) and additional support from the Centre National de la Recherche Scientifique (CNRS). This work was also supported by the ECOS-CONICYT-ANUIES programs through the projects C96U01 and M96U01.

References

Atwater, T., Implications of plate tectonics for the Cenozoic tectonic evolution of western North America, *Geol Soc. Am. Bull.*, *81*, 3513-3536, 1970.

Aubouin, J., J. Bourgois, and J. Azéma, A new type of active margin. the convergent extensional margin as exemplified by the Middle America Trench off Guatemala, *Earth Planet. Sci. Lett.*, *67*, 211-218, 1984

Bangs, N.L., and C. Cande, Episodic development of a convergent margin inferred from structures and processes along the southern Chile margin, *Tectonics*, *16*, 489-503, 1997.

Bangs, N.L., S.C. Cande, S.D. Lewis, and J.J. Miller, Structural framework of the Chile margin at the Chile Ridge collision zone, *Proc. Ocean Drill. Program, Initial Rep.*, *141*, 11-21, 1992.

Barazangi, M., and B. L. Isacks, Spatial distribution of earthquakes and subduction of the Nazca plate beneath South America, *Geology*, *4*, 686-692, 1976

Behrmann, J H., et al., *Proceedings of the Ocean Drilling Program, Initial Reports, vol. 141*, 708 pp, Ocean Drill Program, College Station, Tex, 1992a.

Behrmann, J. H., S D. Lewis, and ODP Leg 141 Scientific Party, Geology and tectonics of the Chile triple junction, *Eos Trans. AGU, 73*, 404-405, 410, 1992b.

Behrmann, J H, S.D. Lewis, S.C. Cande, and ODP Leg 141 Scientific Party, Tectonic and geology of spreading ridge subduction at the Chile triple junction A synthesis of results from Leg 141 of the Ocean Drilling Program, *Geol. Rundsch., 83*, 832-852, 1994

Bourgois, J, and F. Michaud, Active fragmentation of the North America Plate at the triple junction area off Manzanillo, *Geo-Mar Lett., 11*, 59-65, 1991.

Bourgois, J., Y. Lagabrielle , R Maury, J Le Moigne, P. Vidal, J.M. Cantagrel, and O. Urbina, Geology of the Taitao peninsula (Chile margin triple junction area, 46°-47°S): Miocene to Pleistocene obduction of the Bahia Barrientos ophiolite, *Eos Trans AGU, 73(43), Fall Meet. Suppl.*, 592, 1992.

Bourgois, J., Y. Lagabrielle, J. Le Moigne, O. Urbina, M.C. Janin, and P. Beuzart, Preliminary results of a field study of the Taitao ophiolite (southern Chile): Implications for the evolution of the Chile triple junction, *Ofioliti, 18*, 113-129, 1993.

Bourgois, J., H. Martin, Y. Lagabrielle, J. Le Moigne, and J Frutos Jara, Subduction erosion related to spreading-ridge subduction: Taitao peninsula (Chile margin triple junction area), *Geology, 24*, 723-726, 1996.

Bourgois, J., et al., Bathymetry and seismic reflection imaging of tectonic responses to ridge-transform subduction at the Chile triple junction area (45-48°S), CTJ cruise of the R/V *L'Atalante*, *Eos Trans. AGU, 78(46), Fall Meet. suppl.*, F- 636, 1997.

Cande, S.C , and D.V. Kent, A new geomagnetic polarity time scale for the Late Cretaceous and Cenozoic, *J. Geophys. Res., 97*, 13,917-13,951, 1992.

Cande, S.C., and R.B Leslie, Late Cenozoic tectonics of the southern Chile trench, *J. Geophys. Res., 91*, 471-496, 1986.

Cande, S.C., R.B. Leslie, J.C. Parra, and M. Hodbart, Interaction between the Chile ridge and Chile trench: Geophysical and geothermal evidences, *J Geophys. Res., 92*, 495-520, 1987.

Charlton, T. R., Tectonic erosion and accretion in steady-state trenches, *Tectonophysics, 149*, 233-243, 1988.

Cloos, M., Thrust-type subduction-zone earthquakes and seamount asperities: Physical model for seismic rupture, *Geology, 20*, 601-604, 1992.

Cloos, M., and R. L. Shreve, Shear-zone thickness and the seismicity of Chilean- and Marianas-type subduction zones, *Geology, 24*, 107-110, 1996.

DeLong, S.E., and P.J. Fox, Geological consequences of ridge subduction, in *Island Arc, Deep Sea Trenches, and Back-Arc Basins, Maurice Ewing Ser.*, vol. 1, edited by M. Talwani and W.C. Pitman III, pp. 221-228 AGU, Washington, D.C., 221-228, 1977.

DeMets, C., R. G. Gordon, D. F. Argus, and S. Stein, Current plate motions, *Geophys J. Int., 101*, 425-478, 1990.

Dickinson, W. R., and W.S. Snyder, Geometry of triple junctions related to San Andreas transform, *J. Geophys. Res., 84* , 561-572, 1979.

Forsythe, R.D., and E. Nelson, Geological manifestations of ridge collision: Evidence from the Golfo de Penas-Taitao basin, southern Chile, *Tectonics, 4*, 477-495, 1985.

Forsythe, R. D., E.P. Nelson, M J. Carr, M.E. Kaeding, M. Hervé, C.M. Mpodozis, M.J. Soffia, and S Harambour, Pliocene near trench magmatism in southern Chile· A possible manifestation of ridge collision, *Geology, 14*, 23-27, 1986.

Forsythe, R. D., J. K. Meen, J F. Bender, and D. Elthon, Geochemical data on volcanic rocks and glasses recovered from Site 862: Implications for the origin of the Taitao Ridge, Chile triple Junction region, *Proc. Ocean Drill. Program, Sci. Results,141*, 331-348, 1995

Guivel, C., Y. Lagabrielle, J. Bourgois, R Maury, H. Martin, and S. Fourcade, New geochemical constraints for the origin of ridge-subduction-related plutonic and volcanic suites at the Chile triple junction (Taitao peninsula and Site 862, LEG ODP 141), *Tectonophysics, 311*, 83-111, 1999.

Haeussler, P. J., D Bradley, R. Goldfarb, L. Snee, and C. Taylor, Link between ridge subduction and gold mineralization in southern Alaska, *Geology, 23*, 995-998, 1995.

Herron, E. M., S C. Cande, and B. Hall, An active spreading center collides with a subduction zone: A geophysical survey of the Chile margin triple junction, *Mem. Geol. Soc Am., 154*, 683-701, 1981.

Hervé, M., J. Fuenzalida, E. Araya, and A. Solano, Edades radiometricas y tectonica Neogena en el sector costero de Chiloe continental, Xa region, paper presented at *II Congreso Geologico Chileno, Sociedad Geologica de Chile, Arica*, 1979.

Hey, R.N., Speculative propagating rift-subduction zone interactions with possible consequences for continental margin evolution, *Geology, 26*, 247-250, 1998.

Hollin, J.T , and D.H. Schilling, Late Wisconsin-Weichselian mountain glaciers and small ice cap. In *The Last Great Ice Sheets*, edited by G.H. Denton and T.J. Hughes, pp.179-220, John Wiley, New York, 1981.

Hulton, N., D. Sugden, A. Payne, and C. Clapperton, Glacier modeling and climate of Patagonia during the last glacial maximum, *Quat. Res., 42*, 1-19, 1994.

Hussong, D. M., and L. K. Wipperman, Vertical movement and tectonic erosion of the continental wall of the Peru-Chile Trench near 11°30'S latitude, *Mem. Geol. Soc. Am., 154*, 509-524, 1981.

Kaeding, M., R.D. Forsythe, and E.P. Nelson, Geochemistry of the Taitao ophiolite and near trench intrusions from the Chile margin triple junction, *J S. Am Earth Sci , 3*, 161-177, 1990.

Kay, S.M., V A. Ramos, and M. Marquez, Evidence in Cerro Pampa volcanic rocks for slab-melting prior to ridge-trench collision in southern South America, *J. Geol., 101*, 703-714, 1993

Klein, E.M., and J L. Karsten, Ocean ridge basalts with convergent margin geochemical affinities from the southern Chile ridge, *Nature, 374*, 52-57, 1995.

Kulm L.D., et al., *Initial Reports of the Deep Sea Drilling Project, vol. 18*, 1077 pp., U S. Gov. Print Off Washington, D.C., 1973.

Lagabrielle, Y., J. Le Moigne, R. Maury, J. Cotten, and J. Bourgois, Volcanic record of the subduction of an active spreading ridge, Taitao peninsula (southern Chile), *Geology, 22*, 515-518, 1994.

Lallemand, S., and X. Le Pichon, Coulomb wedge model applied to subduction of seamounts in the Japan trench, *Geology, 15*, 1065-1069, 1987.

Le Moigne, J., Y. Lagabrielle, H. Whitechurch, J. Girardeau, J. Bourgois, and R. Maury, Petrology and geochemistry of the ophiolitic and volcanic suites of the Taitao peninsula, Chile triple junction area, *J S. Am Earth Sci , 9*, 43-58, 1996

Leslie, R. B., Cenozoic tectonics of southern Chile: triple junction migration, ridge subduction, and forearc evolution, *Ph.D. thesis*, 276 pp.,*Columbia Univ., New York*, 1986.

Lewis, S.D., J.H. Behrmann, R.J. Musgrave, and S.C. Cande (Eds.), *Proceedings of the Ocean Drilling Program, Scientific Results, vol. 141*, 498 pp., Ocean Drill. Program, College Station, Tex., 1995.

Lowell, T.V., C.J. Heusser, B G. Andersen, P.I. Moreno, A. Hauser, L.E. Heusser, C. Schluchter, D.R. Marchant, and G.H. Denton, Interhemispheric correlation of Late Pleistocene glacial events, *Science, 269*,1541-1549, 1995.

Luhr, J.F., S. Nelson, J.F Allan, and I.S.E. Carmichael, Active rifting in southwestern Mexico· Manifestations of an incipient eastward spreading-ridge jump, *Geology, 13*, 54-57, 1985.

McCarthy, J., and D.W. Scholl, Mechanisms of subduction accretion along the central Aleutian Trench, *Geol. Soc. Am Bull., 96*, 691-701, 1985.

Miller, A , The climate of Chile, in *World Survey of Climatology, vol 12, Climates of Central Chile and South America*, edited by W. Schwerdtferger, pp.113-145, Elsevier, Amsterdam-Oxford-New York, 1976.

Mpodozis, C. M., M. Hervé, C. Nasi, M.J. Soffia, R.D. Forsythe, and E.P. Nelson, El magmatismo Plioceno de peninsula Tres Montes y su relacion con la evolucion del punto triple de Chile austral, *Rev. Geol. Chile, 25-26*, 13-28, 1985.

Murdie, R., D. Prior, P. Styles, S. Flint, R. Pearce, and ⁻ Agar, Seismic responses to ridge-transform subduction. Chile ˛ iple junction, *Geology, 21*, 1095-1098, 1993.

Nelson, E., R. Forsythe, and I. Arit, Ridge collision tectonics in terrane development, *J. S. Am. Earth Sci., 7*, 271-278, 1994

Porter, S.C., C.M. Clapperton, and D.E Sugden, Chronology and dynamics of deglaciation along and near the strait of Magellan, South America, *Sver. Geol. Unders., 81*, 233-239, 1992.

Ramos, V A., and S.M. Kay, Southern Patagonian plateau basalts and deformation: backarc testimony of ridge collision, *Tectonophysics, 205*, 261-282, 1992.

Rohr, K.M.M., and K P. Furlong, Ephemeral plate tectonics at the Queen Charlotte triple junction, *Geology, 23*, 1035-1038, 1995.

Scholl, D.W., Sedimentary sequences in the North Pacific trenches, in

The Geology of Continental Margins, edited by C.A. Burk and C.L. Drake, pp. 493-504, Springer-Verlag, New York, 1974.

Scholl, D.W., R. E. von Huene, T. L. Vallier and D G Howell, Sedimentary masses and concepts about tectonic processes at underthrust ocean margins, *Geology, 8*, 564-568, 1980

Shreve, R.L , and M. Cloos, Dynamics of sediment subduction, melange formation, and prism accretion, *J. Geophys. Res., 91*, 10,229-10,245, 1986.

Sisson, V. B., and T.L. Pavlis, Geologic consequences of plate reorganization: An example from the Eocene southern Alaska forearc, *Geology, 21*, 913-916, 1993

Tebbens, S.F., S C Cande, L. Kovacs, J C. Parra, J L. LaBrecque, and H. Vergara, The Chile ridge: A tectonic framework, *J. Geophys. Res., 102*, 12,035-12059, 1997.

von Huene, R. E , To accrete or not accrete, that is the question, *Geol. Rundch., 75*, 1-15, 1986.

von Huene, R. E., and S Lallemand, Tectonic erosion along the Japan and Peru convergent margins, *Geol Soc. Am Bull., 102*, 704-720, 1990.

von Huene, R. E , and D. W. Scholl, Observations at convergent margins concerning sediment subduction, subduction erosion, and the growth of continental crust, *Rev Geophys., 29*, 279-316, 1991.

Winograd, I.J., J.M. Landwehr, K.R. Ludwig, T.B. Tyler, and A C. Riggs, Duration and structure of the past four interglaciations, *Quat. Res., 48*, 141-154, 1997

J. Boulègue, Laboratoire de Géochimie et Métallogénie, Université Pierre et Marie Curie, Tour 26-16, 5ème étage, Boîte 124, 4 place Jussieu, F-75252 Paris Cedex 05, France. (boulegue@cicrp.jussieu.fr)

J. Bourgois, Centre National de la Recherche Scientifique, Université Pierre et Marie Curie, Laboratoire de Géodynamique, Tectonique et Environnement, Tour 16-26, 4ème étage, Boîte 119, 4 place Jussieu, F-75252 Paris Cedex 05, France. (bourgois@ccr.jussieu.fr)

T. Calmus, Instituto Geologico, Universidad Autonoma de Mexico, Estacion Regional del Noroeste, Hermosillo, Sonora, Mexico. (tcalmus@servidor.unam .mx)

V. Daux, Laboratoire de Géologie Sédimentaire, Université Pierre et Marie Curie, Tour 14-15, 4ème étage, Boîte 117, 4 place Jussieu, F-75252 Paris Cedex 05, France. (daux@ccr jussieu.fr)

C Guivel, Laboratoire de Planétologie et Géodynamique, Université de Nantes, 2 rue de la Houssinière, B.P. 92208, F-44322 Nantes Cedex 3, France. (guivel@chimie.univ-nantes fr)

Y. Lagabrielle, Institut de Recherche pour le Développement, B.P. A5, Noumea Cedex, Nueva Caledonia (lagabrielle@noumea ird.nc)

(Received February 11, 1999; revised August 27, 1999; accepted November 5, 1999.)